NACA TAN TN 01 08




# RESEARCH MEMORANDUM

## A BUFFET INVESTIGATION AT HIGH SUBSONIC SPEEDS OF WING-FUSELAGE-TAIL COMBINATIONS HAVING SWEPTBACK WINGS WITH NACA 64A THICKNESS DISTRIBUTIONS, FENCES, A LEADING-EDGE EXTENSION, AND BODY CONTOURING

By Fred B. Sutton and J. Walter Lautenberger, Jr.

Ames Aeronautical Laboratory
Moffett Field, Calif.

NATIONAL ADVISORY COMMITTEE
FOR AERONAUTICS

WASHINGTON
August 1, 1957
Declassified January 12, 1961

NATIONAL ADVISORY COMMITTEE FOR AERONAUTICS

RESEARCH MEMORANDUM

# A BUFFET INVESTIGATION AT HIGH SUBSONIC SPEEDS OF WING-FUSELAGE-TAIL COMBINATIONS HAVING SWEPTBACK WINGS WITH NACA 64A THICKNESS DISTRIBUTIONS, FENCES, A LEADING-EDGE EXTENSION, AND BODY CONTOURING

By Fred B. Sutton and J. Walter Lautenberger, Jr.

## SUMMARY

An investigation has been made to determine the effect of wing fences, a wing leading-edge extension, changing wing sweepback angle from 40° to 45° and 50°, fuselage contouring, and varying horizontal tail height upon the buffeting response of some typical airplane configurations employing sweptback wings with high aspect ratios. The tests were conducted through an angle-of-attack range at Mach numbers varying from 0.60 to 0.92 at a Reynolds number of 2 million.

For the combinations with 40° of sweepback, the addition of wing fences usually decreased the intensity of buffeting at moderate and high lift coefficients, and reduced the erratic variations of buffeting intensity with increasing lift coefficient and Mach number. Fuselage contouring also reduced buffeting, but was not as effective as wing fences. The leading-edge extension was ineffective as a means of alleviating buffeting and for some test conditions caused increases in buffeting. Increasing the angle of sweepback of the wing from 40° to 45° and 50° usually reduced buffeting at moderate lift coefficients at high subsonic speeds.

At high subsonic Mach numbers, heavy buffeting usually occurred at lift coefficients which were considerably lower than the lift coefficients for pitch-up. The addition of wing fences increased both the lift coefficients for pitch-up and heavy buffeting; however, heavy buffeting still occurred at lift coefficients which were significantly lower than those for pitch-up. Also, at these Mach numbers, the boundaries for light buffeting approximated the lift coefficient and Mach number boundary for drag divergence.

For most test conditions and model configurations, the root-mean-square and the maximum values measured for relative buffeting indicated similar effects and trends; however, the maximum buffeting loads were usually two to three times the root-mean-square intensities.

Increasing the height of the horizontal tail increased tail buffeting at low to moderate lift coefficients, but reduced tail buffeting at moderately high lift coefficients.

## INTRODUCTION

The performance requirements of long-range aircraft designed to fly at high subsonic speeds have usually resulted in configurations which employ sweptback wings of relatively high aspect ratio, and the research described in references 1 through 3 was directed toward the development of satisfactory aerodynamic characteristics for such wings. The wings used in the reference investigations generally experienced, at moderate lift coefficients and high subsonic speeds, a severe decrease in longitudinal stability and heavy buffeting due to shock-induced separation. It was shown by the reference investigations that the lift coefficients at which instability occurred could be increased considerably by the use of chordwise wing fences or leading-edge extensions. However, the effect of such devices on the buffet characteristics of these wings was unknown, and it was believed some of the benefits derived from their use would be at least partially nullified because of heavy buffeting.

The present investigation was conducted to obtain an indication of the effects of a leading-edge extension and multiple chordwise fences on the buffet characteristics of some typical airplane configurations employing sweptback wings of high aspect ratio. In addition to these devices, configurations tested included a Küchemann type fuselage modification, two vertical locations of the horizontal tail, and wing sweepback angles of $40^\circ$, $45^\circ$, and $50^\circ$. Longitudinal force data and fluctuations of wing-root and horizontal tail-root bending moment were measured at Mach numbers up to 0.92 at a Reynolds number of 2 million.

## NOTATION

All areas and dimensions used in the notation refer to the wings without leading-edge extensions.

A aspect ratio, $\frac{b^2}{2S}$

a mean-line designation, fraction of chord over which design load is uniform

a' normal acceleration

BM bending moment

$\frac{b}{2}$ wing semispan perpendicular to the plane of symmetry

$C_D$ drag coefficient, $\frac{\text{drag}}{qS}$

$C_L$ lift coefficient, $\frac{\text{lift}}{qS}$

$C_{L_i}$ inflection lift coefficient, lowest positive lift coefficient at which $\frac{dC_m}{dC_L} = 0$

$C_m$ pitching-moment coefficient about the quarter point of the wing mean aerodynamic chord, $\frac{\text{pitching moment}}{qS\bar{c}}$

$\Delta C_N$ fluctuating normal-force coefficient

c local chord parallel to the plane of symmetry

c' local chord perpendicular to the wing sweep axis

$\bar{c}$ mean aerodynamic chord, $\frac{\int_0^{b/2} c^2 dy}{\int_0^{b/2} c\, dy}$

$c_{l_i}$ section design lift coefficient

g acceleration factor due to gravity

l.e. leading edge

M free-stream Mach number

n normal acceleration factor, $\frac{a'}{g}$

q free-stream dynamic pressure

R Reynolds number based on mean aerodynamic chord of wing

$S$ area of semispan wing

$x$ distance from the intersection of the leading edge of the wing and the plane of symmetry to the moment center, measured parallel to the fuselage center line

$y$ lateral distance from plane of symmetry

$z$ wing height from the quarter point of the mean aerodynamic chord to the fuselage center line, measured in a plane parallel to the plane of symmetry

$\alpha$ angle of attack, measured with respect to a reference plane through the leading edge and root chord of the wings

$\gamma$ ratio of measured damping to critical damping

$\xi$ streamwise distance from the junction of the leading edge of the $45^{\circ}$ sweptback wing with the basic fuselage, dimensionless with respect to the wing chord at the juncture

$\varphi$ angle of twist, the angle between the local wing chord and the reference plane through the leading edge and the root chord of the wing (positive for washin and measured in planes parallel to the plane of symmetry)

$\eta$ fraction of semispan, $\frac{y}{b/2}$

$\Lambda$ angle of sweepback of the line through the quarter-chord points of the reference sections

$\lambda$ wing taper ratio, $\frac{c_t'}{c_r}$

Subscripts

$A$ aerodynamic

$r$ wing root

$rms$ root mean square

$s$ structural

$t$ tail

t' wing tip

T total

## MODEL DESCRIPTION

The wing-fuselage-tail combinations employed the semispan twisted and cambered wing, fuselage, and horizontal tail described in references 1 and 2. For the present investigation, these components were assembled with the root chord of the wing near the center line of the fuselage at an angle of incidence of about 3°. (See fig. 1(a).)

The wing employed sections derived by combining an NACA 64A thickness distribution with an $a = 0.8$ modified mean line having an ideal lift coefficient of 0.4. These sections were perpendicular to the quarter-chord line of the wing panel and had thickness-chord ratios which varied from 14 percent at the root to 11 percent at the tip. Twist was introduced by rotating the streamwise sections of the wing with 40° of sweepback about the leading edge while maintaining the projected plan form. The variations of twist and thickness ratio along the semispan of the unmodified wing are shown in figure 1(b). The sweepback angle of the wing could be set at 40°, 45°, and 50° resulting in respective aspect ratios of about 7, 6, and 5. The leading-edge extension used in the investigation projected 15 percent of the chord ahead of the leading edge of the wing and extended from 60 percent of the wing span to the wing tip. The wing was also tested with multiple fences which were mounted at 33, 50, 70, and 85 percent of the semispan and extended from 10 percent of the chord ahead of the leading edge to the trailing edge. The wing fences and the leading-edge extension are shown in figures 1(c) and 1(d), and are described in detail in references 2 and 3, respectively. The wing was constructed of solid steel, weighed about 375 pounds, and had a fundamental bending frequency of about 15.9 cycles per second. The fences had no appreciable effect on these characteristics; however, the leading-edge extension increased the weight of the wing about 14 pounds and decreased the frequency of fundamental bending to about 15 cycles per second.

The horizontal tail had an aspect ratio of 3.0, a taper ratio of 0.5, NACA 0010 thickness distributions perpendicular to the quarter chord, and 40° of sweepback. It was mounted either on the fuselage center line or at 10.6 inches above the fuselage center line at an angle of incidence of -4°. The tail was constructed of solid steel.

For the present investigation, the wing and tail were weakened locally near the roots to increase the stress level in bending (see fig. 1(e)). Strain-gage bridge elements oriented to respond primarily to bending about an axis perpendicular to the elastic axis were installed on the weakened portions.

The fuselage was assembled with either a cylindrical or an axisymmetric indented midsection with simple fairings fore and aft. The contours of the indented fuselage were determined by the Küchemann technique described in reference 4, and the modification is described in detail in reference 5. The coordinates for the basic fuselage are listed in table I and details of the contoured portion of the fuselage are shown in figure 1(f). The fuselage was relieved at the wing-fuselage juncture and the resultant gap sealed with sponge rubber to maintain an air seal yet minimize mechanical restraint of the wing by the fuselage.

Figure 2 is a photograph of the model mounted in the wind tunnel. The turntable upon which the model was mounted is directly connected to the balance system.

## APPARATUS

The investigation was conducted in the Ames 12-foot pressure wind tunnel which has a contraction ratio of 25 to 1 and eight fine wire mesh screens upstream of the test section. These combine to effect an unusually low turbulence level and hence minimize the possibility of tunnel stream disturbances affecting the test results (see ref. 6).

The static aerodynamic forces and moments were measured with the scale-balance system usually employed for semispan tests, and the steady-state and fluctuating bending moments of the wing and horizontal tail were measured with strain gages installed on the weakened portions of these surfaces.

Preliminary tests indicated that the peak values of the fluctuating bending moments could be used as a measure of buffeting if data samples long enough to provide maximum peak values could be measured for each test condition. Consequently, electronic instrumentation was constructed which conveniently recorded and analyzed data samples corresponding to several thousand cycles of bending moment. This apparatus provided the largest peak values of successive 10-second samples of data, the root-mean-square signal levels of the fluctuations of wing bending moment, and the steady-state wing and tail bending moments. These values were recorded with a multichannel recording potentiometer. Peak values were determined with diode-capacitor circuits. The capacitors were charged to values proportional to the largest signal input. Steady-state values were obtained by sending the signals through low-pass filters to remove the fluctuating portions of the signals. Root-mean-square values were measured with a thermocouple meter element which drove a selsyn unit.

A typical data sample from the recording analyzer is shown in figure 3. Buffeting response was determined from the difference between the maximum fluctuations of bending moment and the average bending moments

or the difference between the rms bending moment and the rms zero. The bridge outputs were also tape recorded for selected test conditions for the later determination of frequency spectrums.

The instrumentation for measuring maximum fluctuating and steady-state signals was calibrated by applying static bending loads to the wing and tail. The resulting calibrations of the channels for measuring the maximum signals were assumed to apply to dynamic loads. The root-mean-square data channel for the wing was calibrated by vibrating the wing with an electromagnetic shaker at its natural frequency for several inputs of constant amplitude while recording the root-mean-square and maximum (peak) signals. A comparison of these signals provided an rms calibration.

## REDUCTION OF DATA

The fluctuations of bending moment measured at the wing root have been converted into fictitious fluctuating normal-force coefficients, $\pm\Delta C_N$, to provide an indication of the relative wing normal force response of the various configurations to buffet. These values were computed from the following relations:

$$\pm\Delta C_N = \frac{\Delta BM}{qS}\frac{1}{y'}$$

where

$\Delta BM$ fluctuating bending moment

$y'$ $\dfrac{\text{steady-state bending moment}}{C_L qS(\cos\alpha) + C_D qS(\sin\alpha)}$

These coefficients correspond to the incremental normal force which, if applied to the wing as a steady load at the lateral position of center of steady-state load, would produce a bending moment of the same magnitude as the measured fluctuating bending moment. The following assumptions were necessary for the calculations. It was assumed that the bending-moment fluctuations at the wing root were not affected by wind-tunnel turbulence and were entirely due to separated flow on the wing. This was substantiated by the negligible fluctuations of wing bending moment near zero lift at most Mach numbers. It was also assumed that the centers of pressure of the wings computed for steady-state conditions applied to fluctuating loads. This assumption was supported by flow studies of the basic wings (see ref. 1) which indicated that shock-induced separation was generally centered near the centers of pressure. This assumption might be less

valid for configurations where the buffeting occurred either inboard or outboard of the center of pressure. Another assumption made for the calculations of fluctuating normal-force coefficient was that the lift of the wing-fuselage-tail combinations at positive angles of attack was close to the lift of the exposed portion of the wing. This assumption is reasonable because of the proximity of the strain-gage bridge used to measure wing bending moments (see fig. 1(e)) to the model plane of symmetry and the negative angle of the fuselage ($-3^{\circ}$) for zero angle of attack of the wing.

Fluctuating normal-force coefficients were computed from both maximum and root-mean-square intensities of wing root bending moment. For maximum loads, the coefficients, $\pm\Delta C_{N_{max}}$, were determined from the largest recorded fluctuations of wing bending moment. Fluctuating normal-force coefficients for the root-mean-square values of the buffet loads, $\pm\Delta C_{N_{rms}}$, were computed from the average of the values recorded after the instrumentation had stabilized for a particular test condition.

The structural and aerodynamic damping ratios of the wing were also determined. These characteristics and the methods used to calculate them are discussed in the appendix.

Fluctuations of tail bending moment, $\pm\Delta BM_t$, measured as an indication of tail buffet are presented as such, and represent the largest fluctuations recorded for the tail.

## CORRECTIONS

The data have been corrected for constriction effects due to the presence of the tunnel walls by the method of reference 7, for tunnel-wall interference originating from lift on the model by the method of reference 8, and for drag tares caused by aerodynamic forces on the turntable upon which the model was mounted.

The corrections to dynamic pressure, Mach number, angle of attack, drag coefficient, and to pitching-moment coefficient were the same as those used for references 2, 3, and 5 and are listed in table II.

No corrections were made to the buffet data for tunnel resonance effects or for tunnel noise as the fluctuations of wing bending moment measured near zero lift were usually negligible.

## RESULTS AND DISCUSSION

### General Remarks

The results presented herein for buffeting may have been influenced by several extraneous factors. In addition to possible discrepancies arising from the conversion of the bending-moment fluctuations to $\pm\Delta C_N$, there would be large differences between the mass and stiffness distribution and the damping characteristics (see the appendix) of the model wings and similar full-scale wings. Also it should be emphasized that values of $\pm\Delta C_n$, as presented herein, are only proportional to the buffeting response of the wing and are undoubtedly larger than the actual fluctuations of aerodynamic normal force causing the buffeting. This difference stems from the relationship between the resonance characteristic of the wing and the frequency of the fluctuating air loads. In addition, reference 9 indicates that the test results may have been affected by the comparatively low Reynolds number (2 million) at which they were obtained.

With the semispan model technique used for this investigation, the pitch and roll motions which can be troublesome with sting-mounted models (see ref. 10) were insignificant. The buffet response of the semispan models was almost entirely limited to the primary bending frequency of the wings and was very similar in this respect to the response of a full-scale airplane (see ref. 11). A typical model frequency spectrum for buffeting conditions is shown in figure 4.

Consideration of these factors indicates that the results can be regarded as a qualitative indication of buffet response for the various configurations tested.

### Discussion of Results

Comparison of maximum and root-mean-square buffet intensities.- The fluctuating normal-force coefficients measured for the various configurations tested are presented in figures 5 through 9. These values are shown for both root-mean-square and maximum intensities. Examination of the results indicates that both criteria generally indicated similar effects and trends. However, it is significant that the maximum buffeting intensities were usually two to three times the root-mean-square intensities. These results are in good agreement with the probability and frequency analysis of buffet loads shown in reference 12 and demonstrate the necessity of applying proper statistical factors to root-mean-square loads to obtain reliable estimates of maximum loads.

Effects of modifications with 40° sweptback wings.- The effects of wing fences, a leading-edge extension, and a Küchemann type fuselage

modification on the buffet intensities of the wing-fuselage-tail combination with the low horizontal tail are compared in figures 5, 6, and 7. At most Mach numbers, the wing fences reduced the erratic variation of buffeting with increasing lift coefficient, and decreased buffet intensities at moderate and high lift coefficients. The leading-edge extension was ineffective as a means of reducing buffeting, and for some test conditions increased buffeting. The effect of the additional mass at the wing tip due to the presence of the extension is not known. However, it is believed to be small and reference 13 shows that this effect, if any, would act to reduce buffeting.

Some unpublished results from flight tests have indicated that in particular instances buffeting originated from interference effects at the intersection of a swept wing and a fuselage. Consequently, the combination with 40° of sweepback was tested with a fuselage modification which was designed to reduce these interference effects (refs. 4 and 5). It is shown in figure 7 that the modification reduced buffeting at most lift coefficients. However, it was not as effective in this respect as the wing fences. This result might have been influenced by the inboard location of the modification. The combination with the modified fuselage was also tested with fences to determine if the beneficial effects of these devices were cumulative. The results of these tests are also shown in figure 7. A comparison of the data presented in this figure and in figures 5 and 6 show no appreciable cumulative effect; the buffet levels measured for the model with wing fences and a modified fuselage were comparable to those measured for the combination with the unmodified fuselage and fences.

Effects of sweepback.- The buffet intensities, with and without wing fences, of wing-fuselage-tail combinations having wings swept 45° and 50° and the tail in the low position are shown in figures 8 and 9, respectively. A comparison of the data presented in these figures, with the data of figures 5 and 6, shows that at moderate lift coefficients the intensity of buffet and the beneficial effect of wing fences on these intensities decreased with increasing angle of sweepback. These results might have been anticipated and probably stem from reductions in compressibility effects which accompanied the change in sweepback angle.

Tail buffet.- Figures 10 and 11 show, for the combination with 40° of sweepback, the effect of wing fences, a fuselage modification, and tail height on tail buffeting as indicated by the fluctuating bending moments measured at the root of the horizontal tail. Because of the erratic nature of the data, no noticeable trend was evident from the addition of wing fences or from modifying the fuselage (fig. 10). However, the data of figure 11 show that changing to the higher tail usually increased the magnitude of the bending-moment fluctuations at low to moderate lift coefficients and reduced these fluctuations at moderately high lift coefficients. The data showing the effects of tail height (fig. 11) were obtained from tests of the combination with the leading-edge extension on the wing while

the data showing the effects of the other configuration changes (fig. 10) were measured with the extension removed. This probably accounts for the small discrepancies between the low tail data of figure 11 and the basic wing, basic fuselage data of figure 10.

Static force data.- Static longitudinal force data for the various combinations with 40° of sweepback and the low horizontal tail position are presented in figures 12 and 13. Figure 14 shows these data for the combinations with 45° and 50° of sweepback. No static force data are presented for the combination with the high tail since, for the range of conditions investigated, the effect of raising the tail on the static characteristics of the model was small (see ref. 2).

Buffet boundaries.- Figures 15 through 18 present lift coefficient and Mach number boundaries for constant-intensity buffeting. A few root-mean-square measurements of relatively low intensity buffet were not obtained because of instrumentation difficulties. These conditions are indicated in figure 16(a) by the short dashed lines which were used to connect the available data points.

The relative effects of wing fences, a wing leading-edge extension, and a fuselage modification on boundaries for buffeting of comparatively moderate intensity are compared in figure 15 for the combination with 40° of sweepback. Over most of the Mach number range, the buffet boundary for the combination with fences was at the highest lift levels. The buffet characteristics of the combination with and without wing fences are shown in detail in figure 16 by boundaries for constant buffeting intensities which range from the first perceptible traces of buffeting to buffeting of extreme degree. The increments of $\pm\Delta C_N$ (0.005 for root-mean-square values and 0.01 for maximums) chosen for these plots were not intended to imply the accuracy or repeatability of the data (which was equivalent to a $\pm\Delta C_{N_{rms}}$ of 0.002 or a $\pm\Delta C_{N_{max}}$ of about 0.005), but were only selected to convey the extremely erratic nature of the buffeting of the unmodified wing-fuselage-tail combination. The bubble-like curves are due to decreases in buffeting intensities with increasing lift coefficient or angle of attack. This effect is also shown by the investigation reported in reference 9. Fences usually increased the lift levels for most constant buffeting intensities and somewhat reduced the erratic variation of the maximum intensities with increasing Mach number.

Figure 17 compares for the models with 40°, 45°, and 50° of sweepback, lift coefficient and Mach number boundaries for relatively light, moderate, and heavy intensities of buffeting. Boundaries are shown for the model with and without wing fences. Although these data are relatively erratic, it is indicated that for the selected buffeting intensities increasing sweepback usually raised the lift level of the buffet boundaries at the higher test Mach numbers.

Comparison of buffet boundaries with static longitudinal parameters.- The lift coefficients for drag divergence ($C_L$ for $dC_D/dM = 0.10$) and for pitching-moment curve inflection or pitch-up (lowest positive $C_L$ at which $dC_m/dC_L = 0$) have often been considered important design parameters in analyzing the static longitudinal characteristics of airplanes for flow separation. These parameters are compared in figure 18 with Mach number and lift coefficient boundaries for light and heavy buffeting. The intensity selected for light buffeting, $\pm\Delta C_{N_{max}} = 0.02$, is believed to approximate the buffet onset criteria used for full-scale airplanes. The intensity chosen for heavy buffeting, $\pm\Delta C_{N_{max}} = 0.08$, is purely arbitrary and is only intended to indicate constant-intensity buffeting of relatively heavy degree. At the higher Mach numbers, the lift coefficients for drag divergence are close to the boundaries for light buffeting for both the model with and without wing fences. However, heavy buffeting was indicated at lift coefficients considerably lower than those for moment-curve inflection, and this is significant since the occurrence of heavy buffeting at these comparatively low lift coefficients indicates that the usable range of lift coefficients would probably be much less than the lift coefficient range for stability. Wing fences did much to lessen this difference, but heavy buffeting was still indicated at lift coefficients which were appreciably lower than those for pitch-up.

Hypothetical buffet characteristics of an assumed airplane.- Because of the model stiffness and mode shape limitations mentioned earlier in the paper, no attempt was made to use the scaling relationship presented in references 11 and 14 in analyzing the results. However, incremental values of normal acceleration factor, $\pm\Delta n$, have been calculated for an assumed airplane from some of the response data showing maximum peak values of fluctuating normal-force coefficients, $\pm\Delta C_{N_{max}}$. It was assumed that this airplane had the same geometry and dynamic response characteristics as the model with 40° of sweepback and was in flight at an altitude of 40,000 feet with a wing loading of 70 pounds per square foot. Since the normal acceleration factors, $\pm\Delta n$, were calculated from fictitious normal-force coefficients (see the section on reduction of data), they are subject to the same limitations which affect the absolute magnitude of these normal-force coefficients. However, the presentation in figure 19 of the fluctuations of normal acceleration as a function of Mach number and constant normal acceleration factor emphasizes the alleviating effect of wing fences on buffeting at the higher Mach numbers of the test. Buffeting due to increasing Mach number at constant normal acceleration factor and buffeting due to increases in normal acceleration factor at constant Mach number were greatly reduced by the addition of the fences.

## CONCLUSIONS

An investigation has been made to determine the effect of wing fences, a wing leading-edge extension, wing sweepback angle, fuselage contouring, and horizontal tail height upon the buffeting response of some typical airplane configurations employing swept back wings of high aspect ratio. The following conclusions were indicated:

1. For the combinations with 40° of sweepback, the addition of wing fences usually decreased buffeting at moderate and high lift coefficients, and reduced the erratic variation of buffet intensities with increasing lift coefficient and Mach number. Fuselage contouring also reduced buffeting, but was not as effective as the wing fences. The leading-edge extension was ineffective as a means of alleviating buffeting and for some test conditions increased buffeting.

2. Increasing the angle of sweepback of the wing from 40° to 45° and 50° usually reduced buffeting at moderate lift coefficients at high subsonic speeds.

3. At high subsonic speeds, heavy buffeting was usually indicated at lift coefficients which were considerably lower than the lift coefficients for pitch-up. The addition of wing fences increased both the lift coefficients for pitch-up and for heavy buffeting; however, heavy buffeting still occurred at lift coefficients significantly lower than the lift coefficients for pitch-up.

4. At high subsonic speeds, the boundaries for light buffeting were close to the lift coefficient and Mach number boundary for drag divergence.

5. For most test conditions and model configurations, the root-mean-square and the maximum values measured for relative buffeting indicated similar effects and trends; however, the maximum buffeting loads were usually two to three times the root-mean-square intensities.

6. Increasing the height of the horizontal tail increased tail buffeting at low to moderate lift coefficients, but reduced tail buffeting at moderately high lift coefficients.

Ames Aeronautical Laboratory
National Advisory Committee for Aeronautics
Moffett Field, Calif., June 6, 1957

## APPENDIX

## WING DAMPING CHARACTERISTICS

The damping characteristics of the wing for several test conditions were determined from frequency analyses of the fluctuating wing-root bending moments. Magnetic tape recordings of these moments taken during the test were formed into loops and played into an electrical frequency analyzer having a narrow band-pass filter with a band width of about 1/2 cycle per second. A typical frequency analysis is presented in figure 4 which shows the variation with frequency of the wing structural response. In this case, the response was proportional to inch-pounds instead of the usually used $(\text{inch-pounds})^2$.

The results of these analyses showed that almost all of the response appeared in the first bending mode (see fig. 4) and the following relation from reference 15 was used to obtain an approximation of the total damping ratio, $\gamma_T$, from the response spectrums.

$$\gamma_T = \frac{1}{2} \frac{\Delta\omega}{\omega_N}$$

where

$\gamma_T$ $\quad \dfrac{\text{total damping present}}{\text{critical damping}}$

$\omega_N$ first natural bending frequency, cps

$\Delta\omega$ band width at the half-power points

The half-power points are defined as the points on the response curves where the power is one-half peak power. For example, the half-power points of the curve shown in figure 4 correspond to 0.707 peak amplitude. The damping results obtained with this technique were very erratic because of inherent limitations in the frequency analyzer. For some test conditions, the band width of the half-power points approached the band width of the filter, and for these conditions it was probable that large errors were present in the results. However, when the band width of the half-power point was considerably wider than the band width of the filter, the resulting damping values were believed to be reasonably accurate, and the maximum measured value of total damping thus obtained was of the order of 0.026.

The structural damping ratio of the wing, $\gamma_s$, was determined from the following relationship.

$$e^{-2\pi n'\gamma_s} = \frac{\text{amplitude at cycle } n'}{\text{initial amplitude}}$$

where

$\gamma_s$ $\frac{\text{structural damping}}{\text{critical damping}}$

$n'$ number of cycles (in this case to damp to half amplitude)

The number of cycles to damp to half amplitude, n', was determined by striking the wing and recording the response decay with an oscillograph. The value of $\gamma_s$ thus obtained was 0.0055.

The aerodynamic damping ratio of the wing, $\gamma_a$, was assumed to be the total damping ratio less the structural damping ratio. Consequently, the maximum measured aerodynamic damping ratio was about 0.020.

The analysis of the tapes for several test conditions showed that the first natural bending frequency of the wing varied between 16.9 and 17.6 cycles per second. The static wing natural bending frequency was 15.9 cps. The increase in natural frequency was believed due to the added stiffness contributed by the aerodynamic forces that arise when the wing vibrates in a moving air stream.

## REFERENCES

1. Sutton, Fred B., and Dickson, Jerald K.: A Comparison of the Longitudinal Aerodynamic Characteristics at Mach Numbers Up to 0.94 of Sweptback Wings Having NACA 4-Digit or NACA 64A Thickness Distributions. NACA RM A54F18, 1954.

2. Dickson, Jerald K., and Sutton, Fred B.: The Effect of Wing Fences on the Longitudinal Characteristics at Mach Numbers Up to 0.92 of a Wing-Fuselage-Tail Combination Having a 40° Sweptback Wing With NACA 64A Thickness Distribution. NACA RM A55C30a, 1955.

3. Sutton, Fred B.: The Effect of Leading-Edge Extensions on the Longitudinal Characteristics at Mach Numbers Up to 0.92 of a Wing-Fuselage-Tail Combination Having a 40° Sweptback Wing With NACA 64A Thickness Distribution. NACA RM A55I29, 1956.

4. McDevitt, John B., and Haire, William M.: Investigation at High Subsonic Speeds of a Body-Contouring Method for Alleviating the Adverse Interference at the Root of a Sweptback Wing. NACA TN 3672, 1956. (Supersedes NACA RM A54A22, 1954)

5. Sutton, Fred B., and Lautenberger, J. Walter, Jr.: The Effect of Body Contouring on the Longitudinal Characteristics at Mach Numbers Up to 0.92 of a Wing-Fuselage-Tail and Several Wing-Fuselage Combinations Having Sweptback Wings of Relatively High Aspect Ratio. NACA RM A56J08, 1957.

6. Dryden, Hugh L., and Abbott, Ira H.: The Design of Low-Turbulence Wind Tunnels. NACA Rep. 940, 1949.

7. Herriot, John G.: Blockage Corrections for Three-Dimensional-Flow Closed Throat Wind Tunnels With Consideration of the Effect of Compressibility. NACA Rep. 995, 1950. (Formerly NACA RM A7B28)

8. Sivells, James C., and Salmi, Rachel M.: Jet-Boundary Corrections for Complete and Semispan Swept Wings in Closed Circular Wind Tunnels. NACA TN 2454, 1951.

9. Polentz, Perry P., Page, William A., and Levy, Lionel L., Jr.: The Unsteady Normal-Force Characteristics of Selected NACA Profiles at High Subsonic Mach Numbers. NACA RM A55C02, 1955.

10. Kemp, William B., Jr., and King, Thomas J., Jr.: Wind-Tunnel Measurements of Wing Buffeting on 1/16-Scale Model of Douglas D-558-II Research Airplane. NACA RM L56G31, 1956.

11. Huston, Wilbur B., Rainey, A. Gerald, and Baker, Thomas F.: A Study of the Correlation Between Flight and Wind-Tunnel Buffeting Loads. NACA RM L55E16b, 1955.

12. Huston, Wilbur B., and Skopinski, T. H.: Probability and Frequency Characteristics of Some Flight Buffet Loads. NACA TN 3733, 1956.

13. Huston, Wilbur B., and Skopinski, T. H.: Measurement and Analysis of Wing and Tail Buffeting Loads on a Fighter-Type Airplane. NACA TN 3080, 1954.

14. Skopinski, T. H., and Huston, Wilbur B.: A Semiempirical Procedure for Estimating Wing Buffet Loads in the Transonic Region. NACA RM L56E01, 1956.

15. Scanlan, Robert H., and Rosenbaum, Robert: Introduction to the Study of Aircraft Vibration and Flutter. The MacMillan Co., New York, 1951.

TABLE I.- COORDINATES OF BASIC FUSELAGE

| Distance from nose, in. | Radius, in. | Distance from nose, in. | Radius, in. |
|---|---|---|---|
| 0 | 0 | 60.00 | 5.00 |
| 1.27 | 1.04 | 70.00 | 5.00 |
| 2.54 | 1.57 | 76.00 | 4.96 |
| 5.08 | 2.35 | 82.00 | 4.83 |
| 10.16 | 3.36 | 88.00 | 4.61 |
| 20.31 | 4.44 | 94.00 | 4.27 |
| 30.47 | 4.90 | 100.00 | 3.77 |
| 39.44 | 5.00 | 106.00 | 3.03 |
| 50.00 | 5.00 | 126.00 | 0 |

TABLE II.- CORRECTIONS TO DATA

(a) Corrections for constriction effects

| Corrected Mach number | Uncorrected Mach number | $\frac{q_{corrected}}{q_{uncorrected}}$ |
|---|---|---|
| 0.60 | 0.590 | 1.006 |
| .70 | .696 | 1.007 |
| .80 | .793 | 1.010 |
| .83 | .821 | 1.012 |
| .86 | .848 | 1.015 |
| .88 | .866 | 1.017 |
| .90 | .883 | 1.020 |
| .92 | .899 | 1.024 |

(b) Corrections for tunnel-wall interference

$$\Delta\alpha = 0.455\ C_L$$

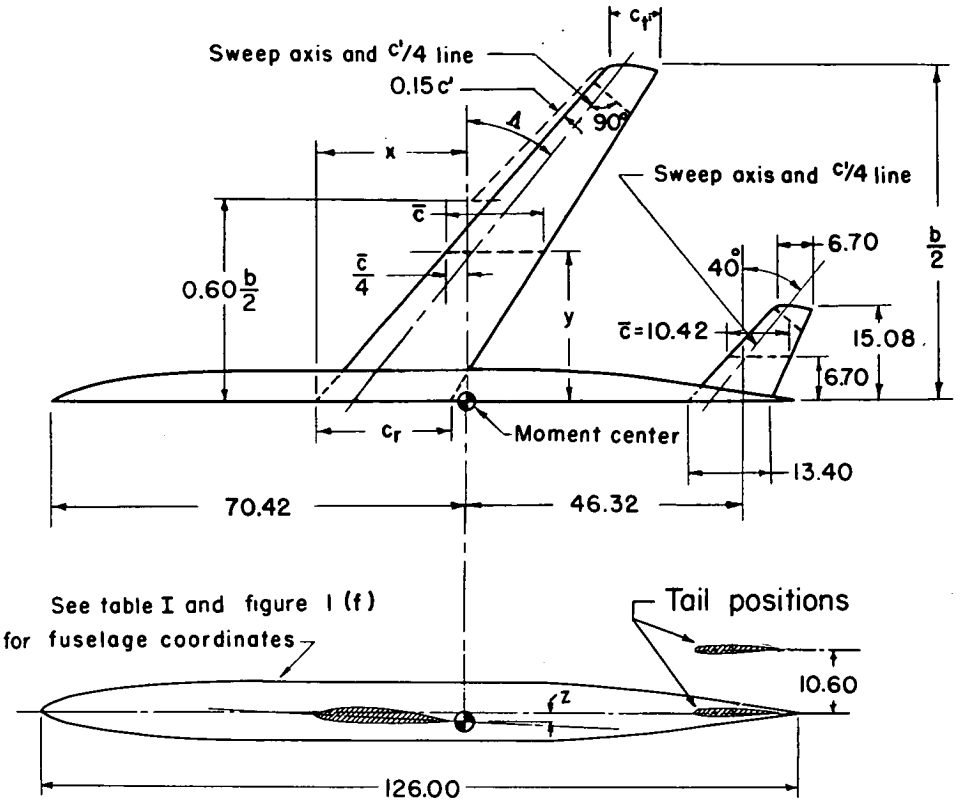
$$\Delta C_D = 0.00662\ C_L^2$$

$$\Delta C_{m_{tail\ off}} = K_1 C_{L_{tail\ off}}$$

$$\Delta C_{m_{tail\ on}} = K_1 C_{L_{tail\ off}} - \left[ (K_2 C_{L_{tail\ off}} - \Delta\alpha) \frac{\partial C_m}{\partial i_t} \right]$$

where:

| M | $K_1$ | $K_2$ |
|---|---|---|
| 0.60 | 0.0038 | 0.74 |
| .70 | .0043 | .76 |
| .80 | .0049 | .79 |
| .83 | .0050 | .80 |
| .86 | .0053 | .83 |
| .88 | .0054 | .84 |
| .90 | .0056 | .86 |
| .92 | .0057 | .88 |

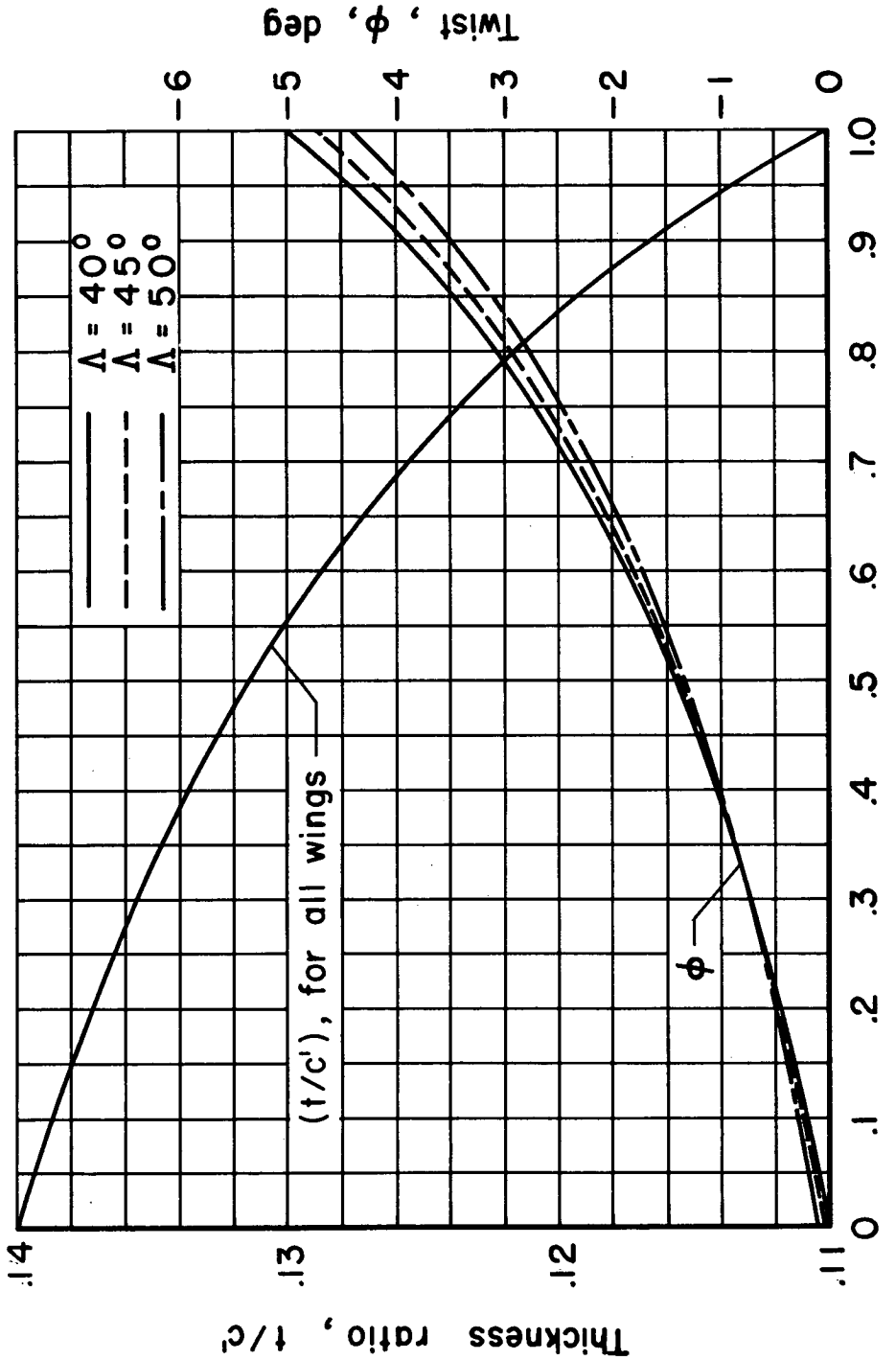



| Geometry of the wings | | | | | | | | | | | |
|---|---|---|---|---|---|---|---|---|---|---|---|
| Λ | A | λ | b/2 | $c_r$ | $c_t'$ | $\bar{c}$ | x | y | z | S | $a_r$ |
| 40° | 7.00 | 0.4 | 54.61 | 22.29 | 8.92 | 16.56 | 25.35 | 23.40 | 1.45 | 5.92 | 3.00° |
| 45° | 6.03 | 0.4 | 50.41 | 23.90 | 9.56 | 17.76 | 27.76 | 21.60 | 1.45 | 5.86 | 2.95° |
| 50° | 5.04 | 0.4 | 45.82 | 25.98 | 10.39 | 19.30 | 30.13 | 19.64 | 1.45 | 5.79 | 2.90° |

Note: All dimensions in inches and areas in square feet.

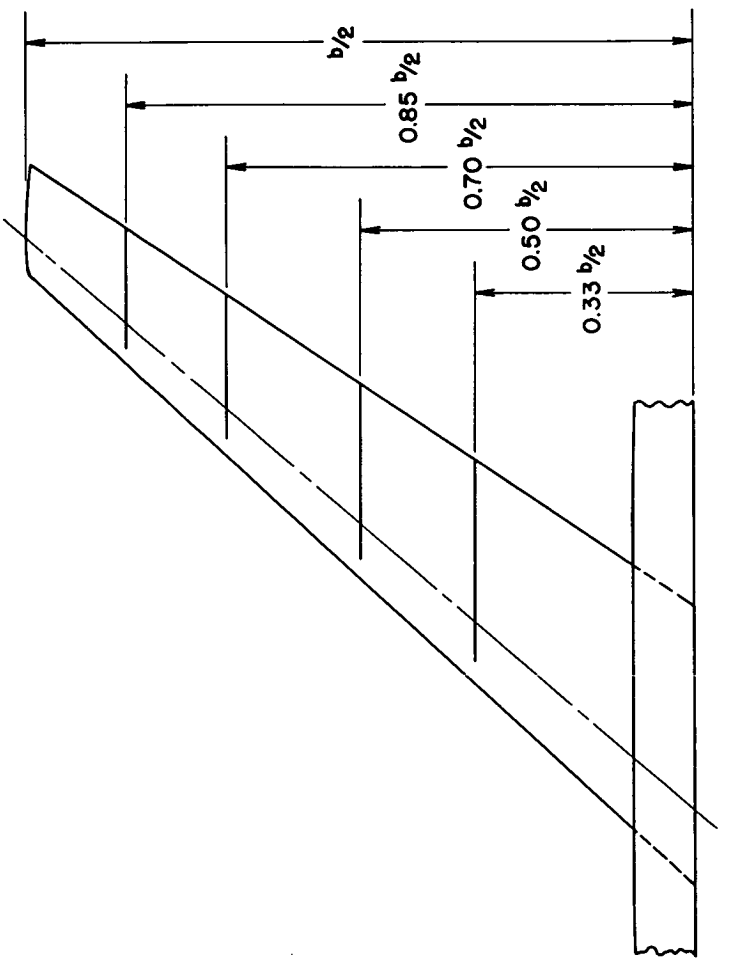
(a) General arrangement.

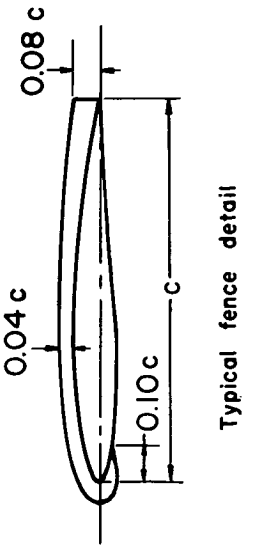
Figure 1.- Geometry of the models.




(b) Distribution of twist and thickness ratio.

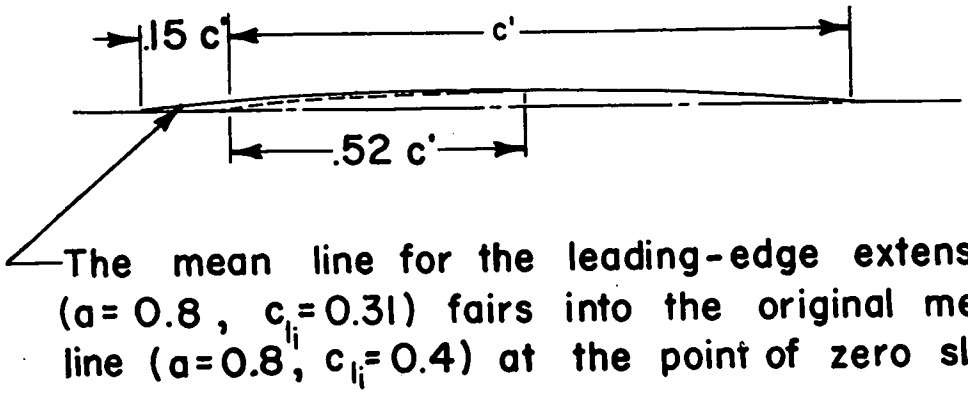
Figure 1.- Continued.

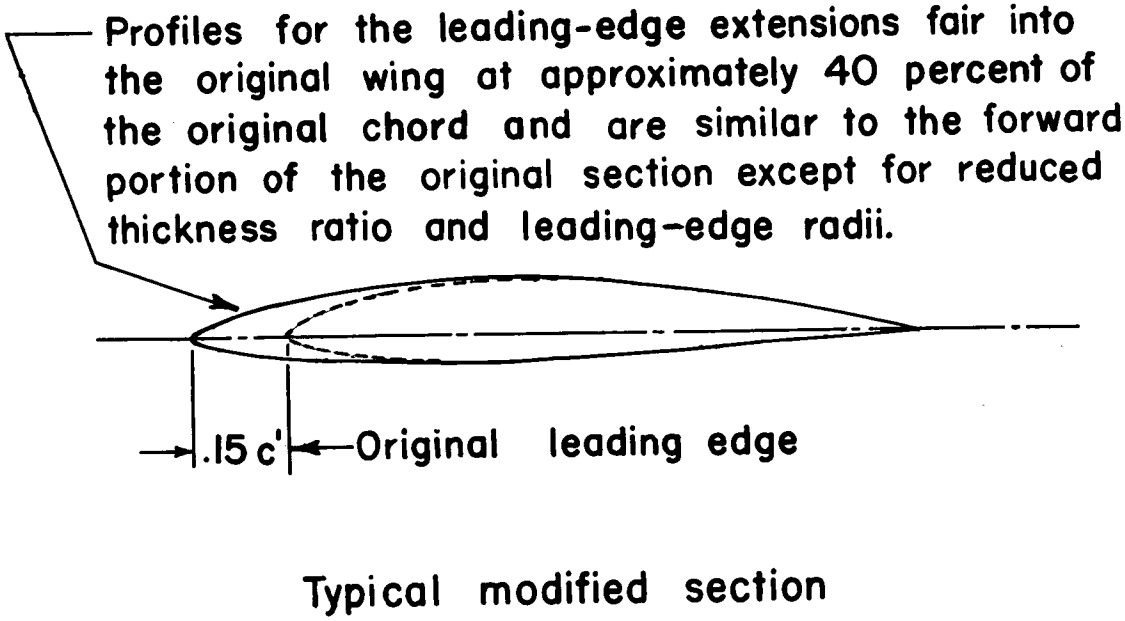



(c) Wing fence details.

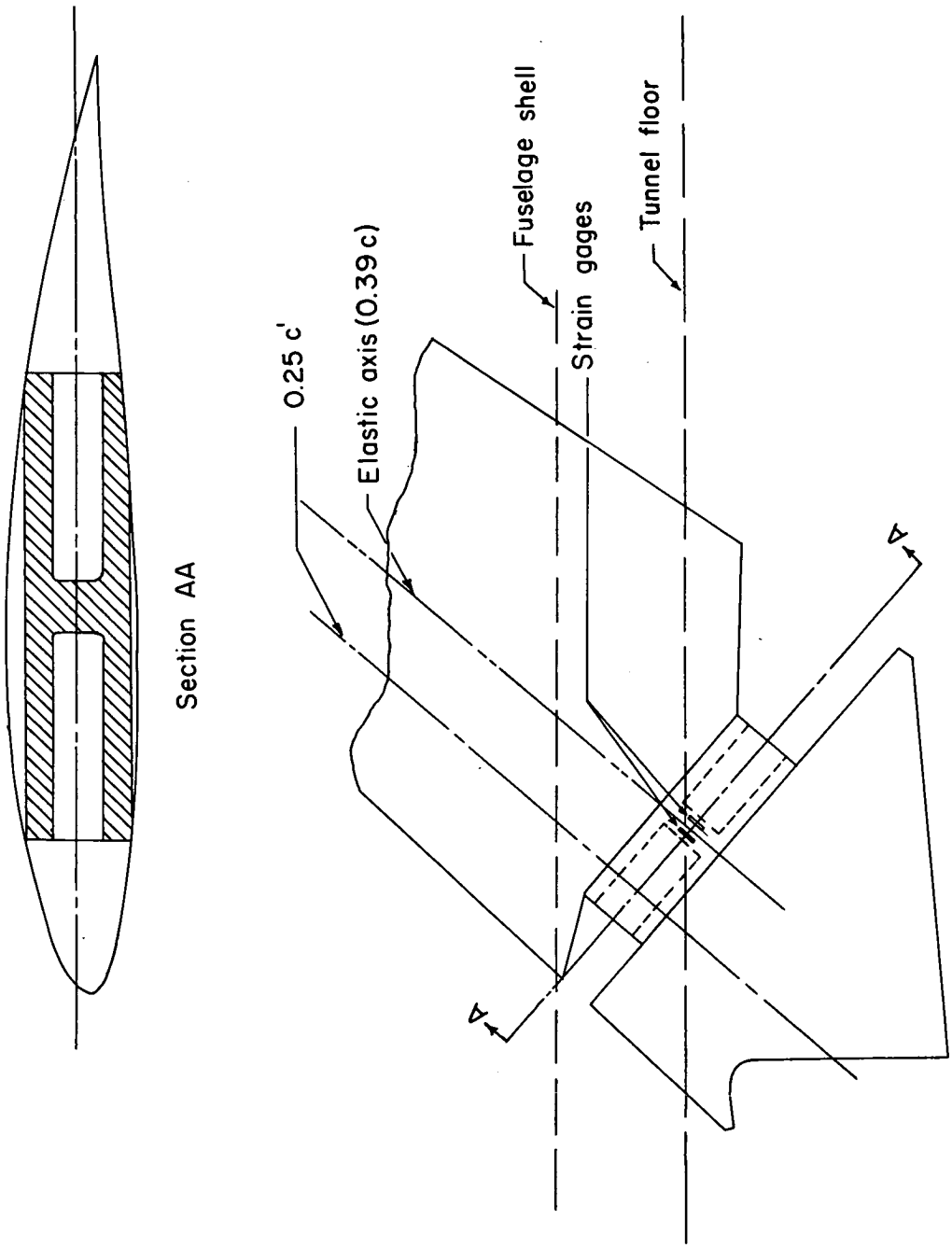
Figure 1.- Continued.



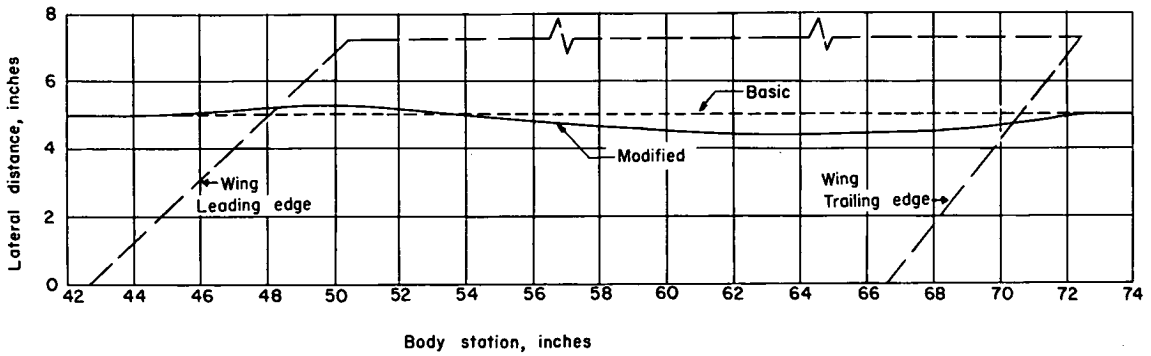

(d) Details of leading-edge extension.

Figure 1.- Continued.




(e) Wing-root detail.

Figure 1.- Continued.




| Body station, inches | $\xi$ | Body radius, inches |
|---|---|---|
| 38.437 | -0.428 | 5.000 |
| 39.437 | -.384 | 5.000 |
| 43.567 | -.2 | 5.000 |
| 45.815 | -.1 | 5.047 |
| 48.063 | 0 | 5.166 |
| 50.311 | .1 | 5.266 |
| 52.559 | .2 | 5.115 |
| 54.806 | .3 | 4.911 |
| 57.054 | .4 | 4.718 |
| 59.302 | .5 | 4.585 |
| 61.550 | .6 | 4.452 |
| 63.798 | .7 | 4.427 |
| 66.045 | .8 | 4.426 |
| 68.293 | .9 | 4.505 |
| 70.541 | 1.0 | 4.799 |
| 72.000 | 1.065 | 4.985 |
| 73.000 | 1.109 | 5.000 |

(f) Fuselage contouring details.

Figure 1.- Concluded.



A-21695

Figure 2.- Photograph of the model in the wind tunnel.

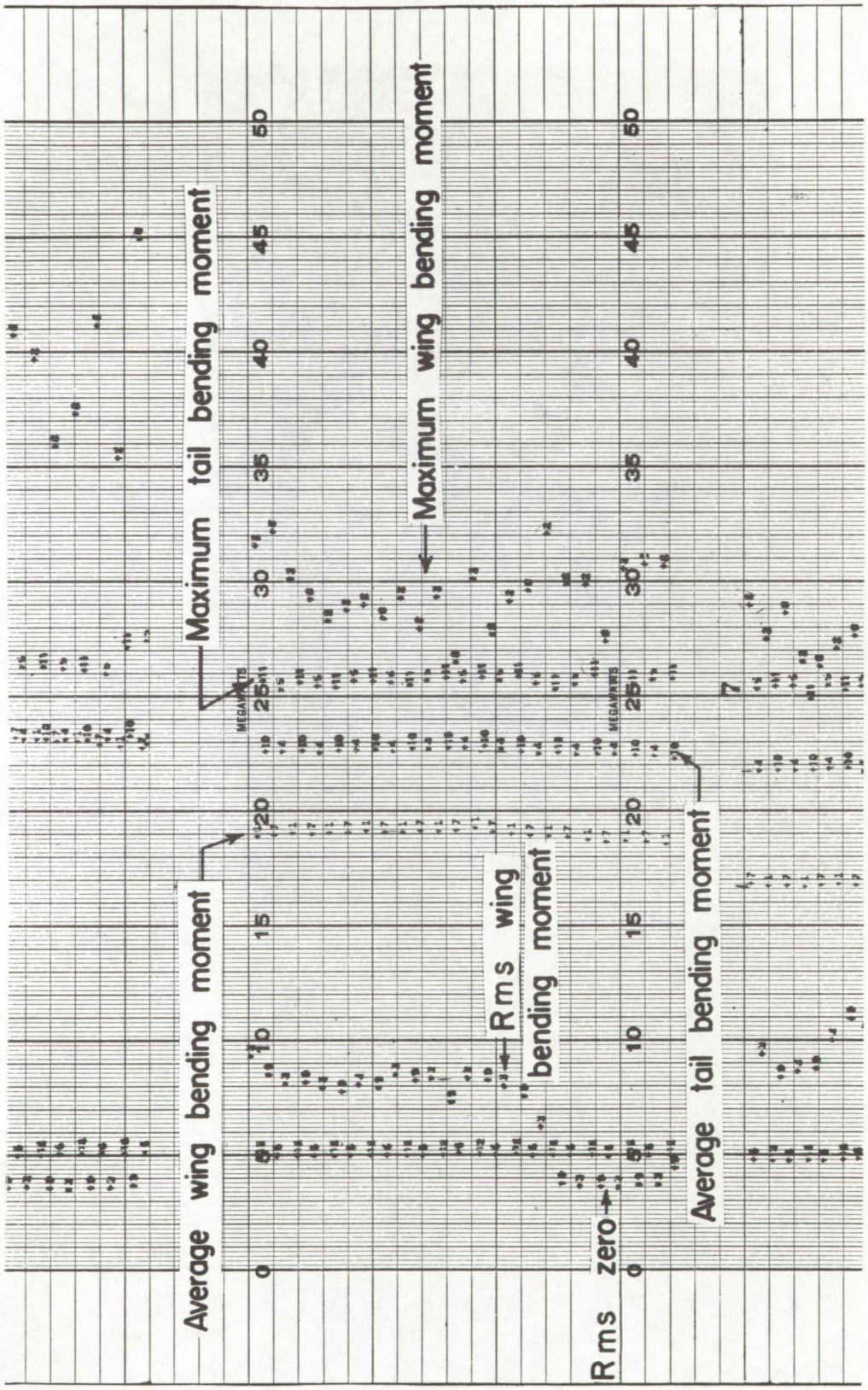



Figure 3.- Sample buffet data records; M = 0.88, $\alpha = 9^{\circ}$.

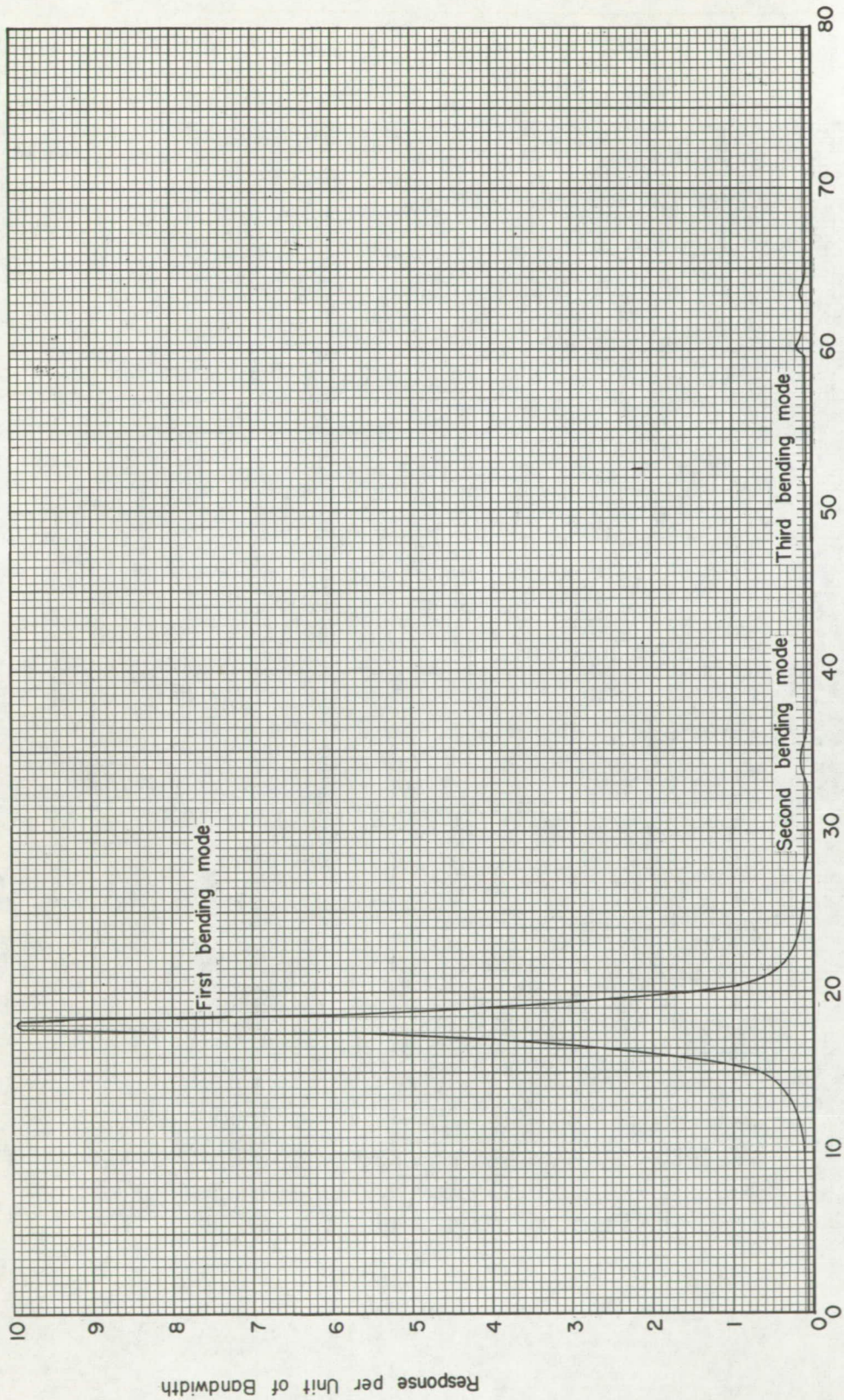
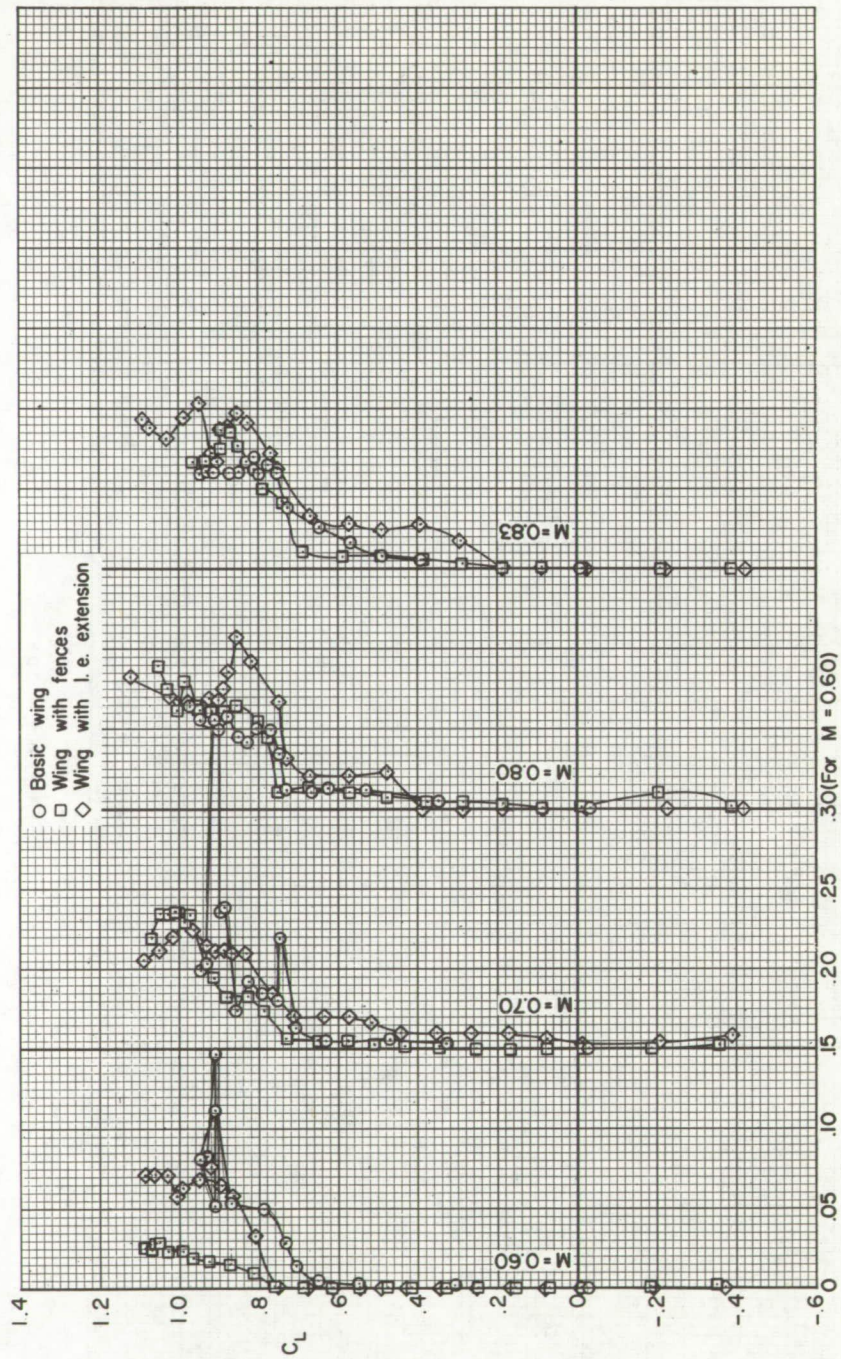
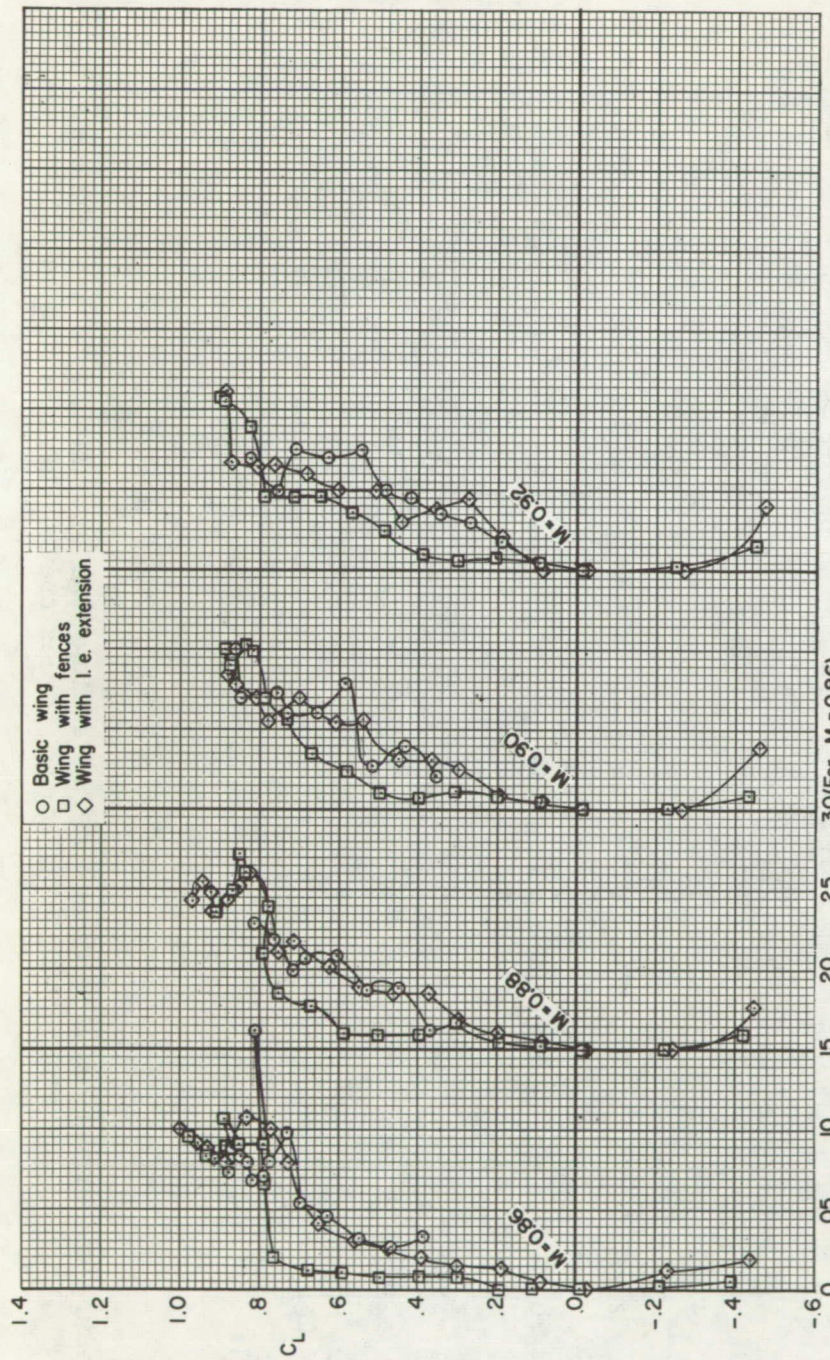



Figure 4.- Typical frequency spectrum for the basic wing-fuselage-tail combination with 40° of sweepback; $M = 0.90$, $\alpha = 8°$.



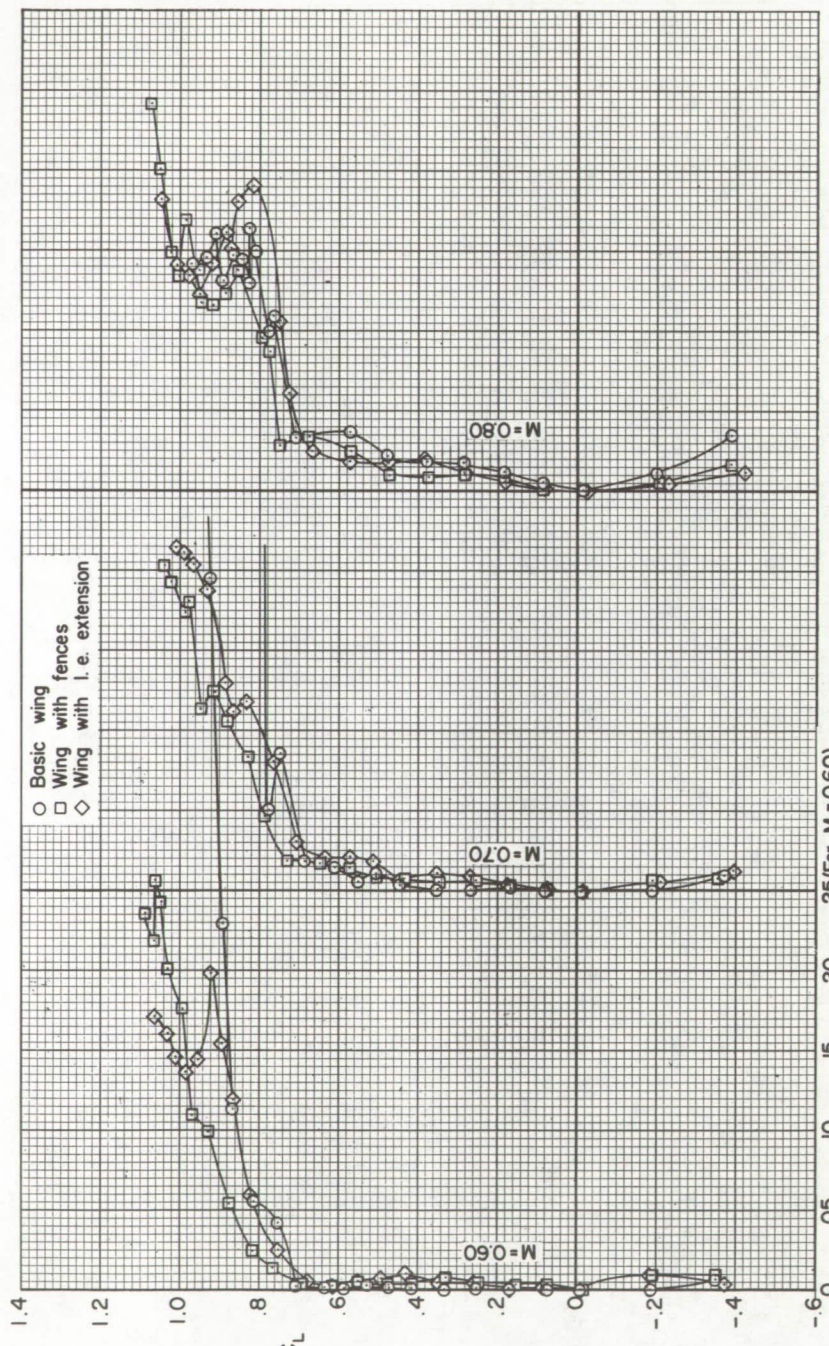

(a) M = 0.60, 0.70, 0.80, 0.83

Figure 5.- The effect of wing fences and a leading-edge extension upon the root-mean-square fluctuations of wing normal forces due to buffet; $\Lambda = 40^{\circ}$.



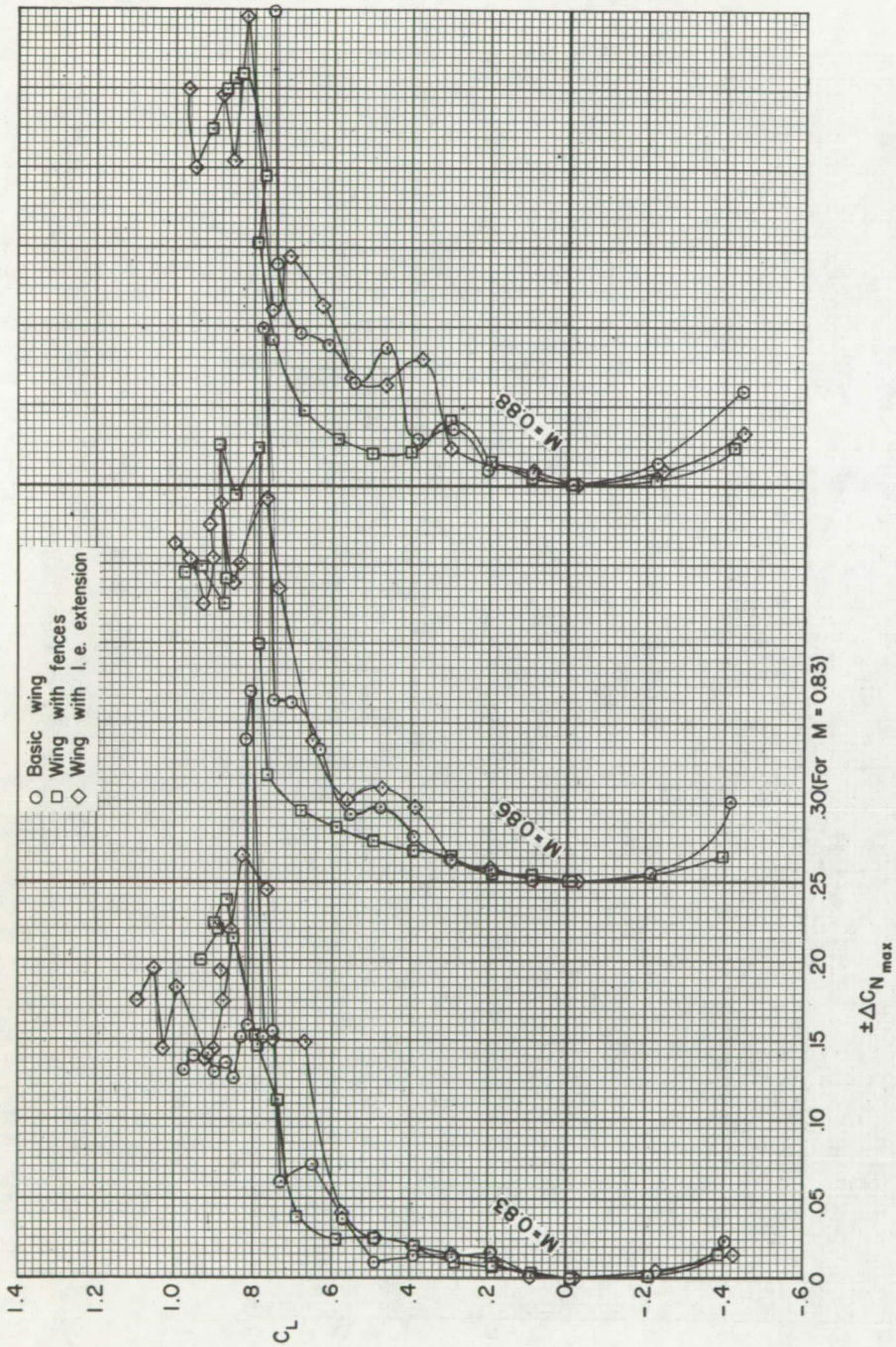

(b) M = 0.86, 0.88, 0.90, 0.92

Figure 5.- Concluded.



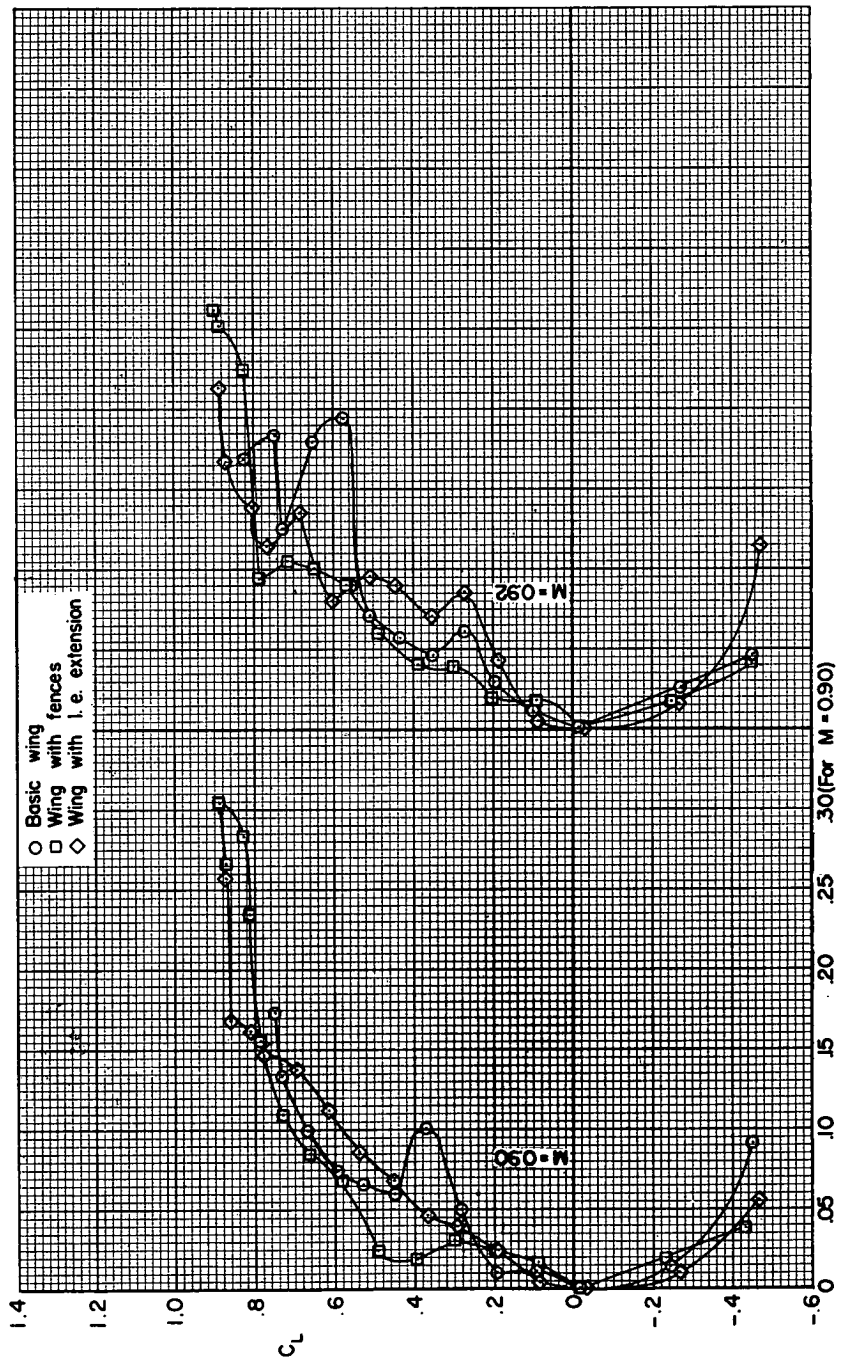

(a) M = 0.60, 0.70, 0.80

Figure 6.- The effect of wing fences and a leading-edge extension upon the maximum intensities of fluctuating wing normal forces due to buffett; $\Lambda = 40^{\circ}$.



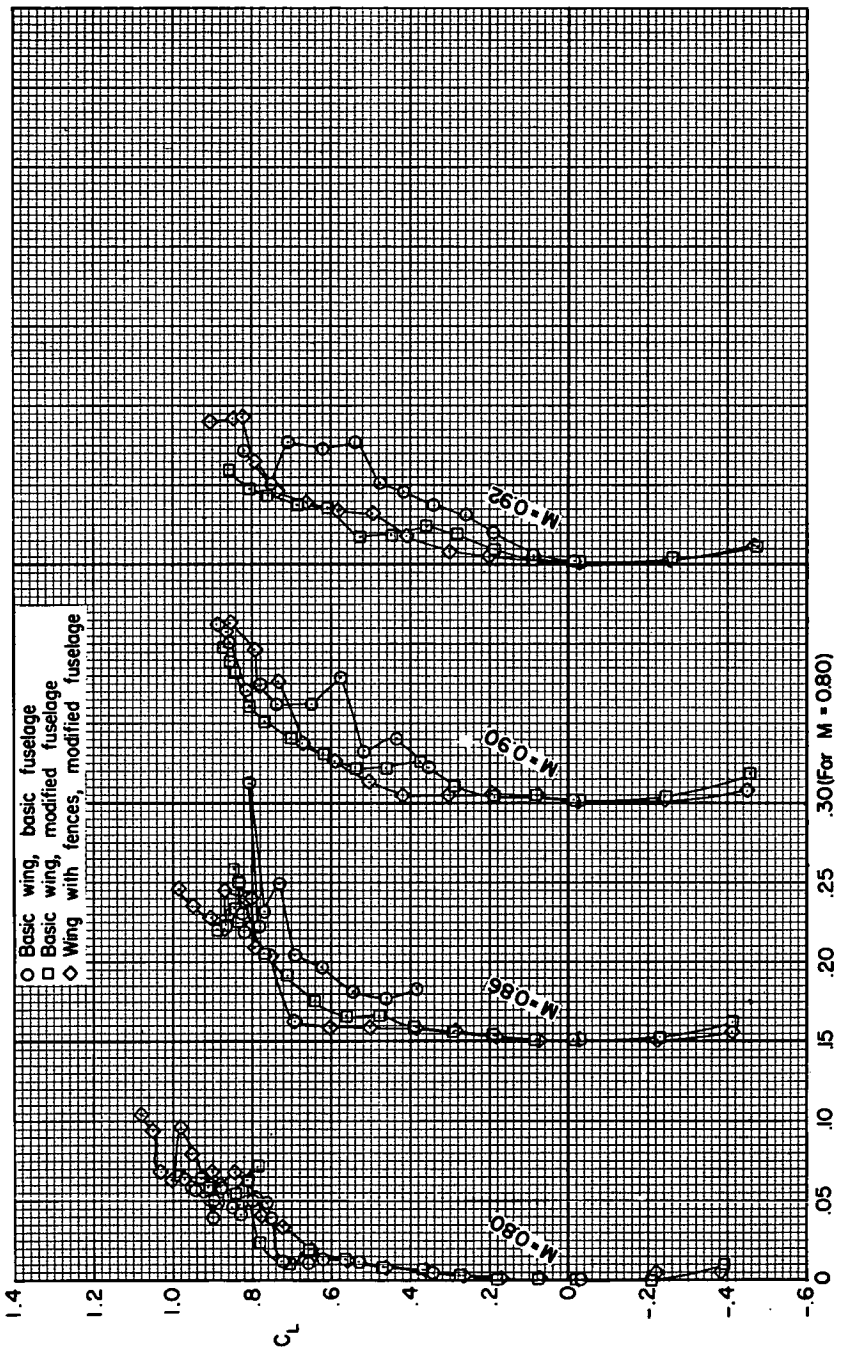

(b) M = 0.83, 0.86, 0.88

Figure 6.- Continued.



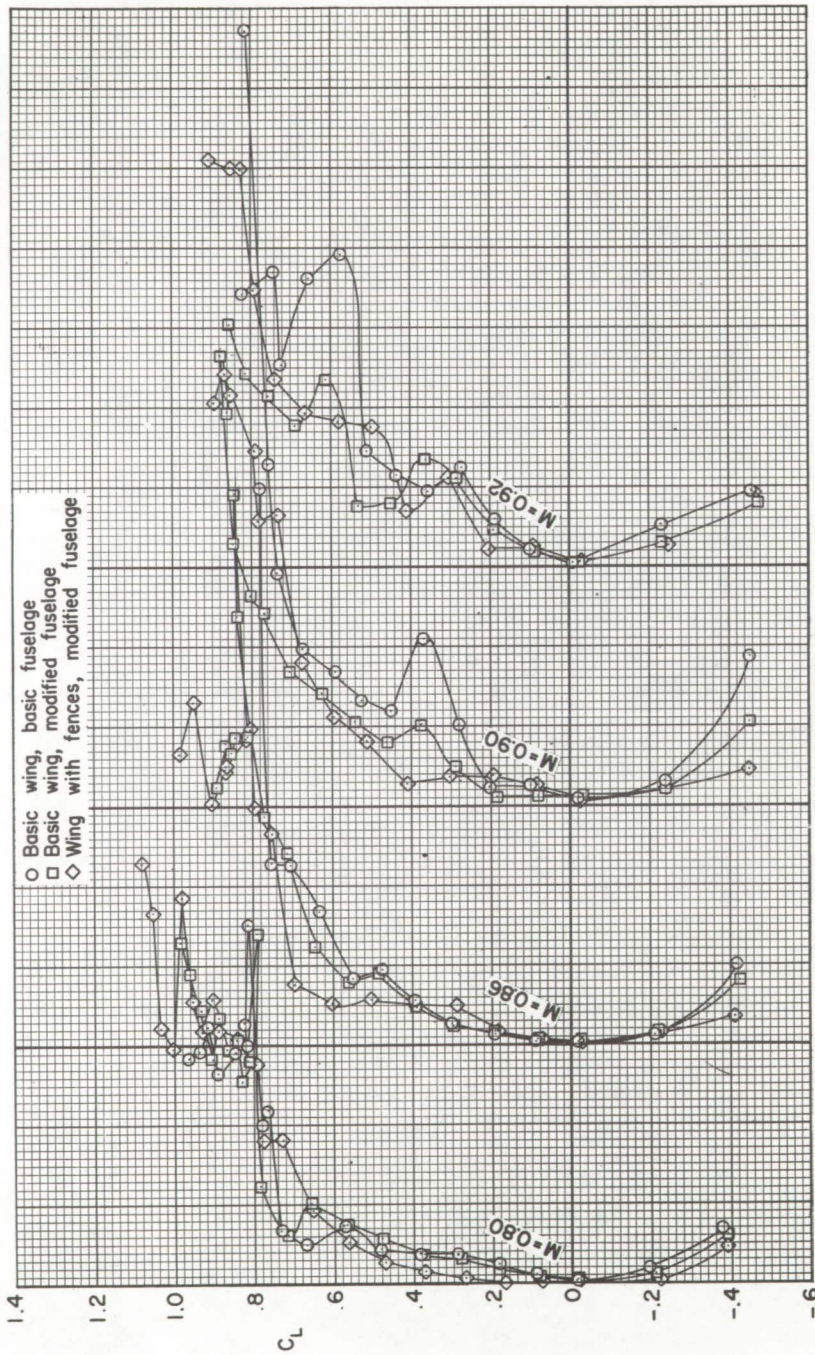

(c) M = 0.90, 0.92

Figure 6.- Concluded.



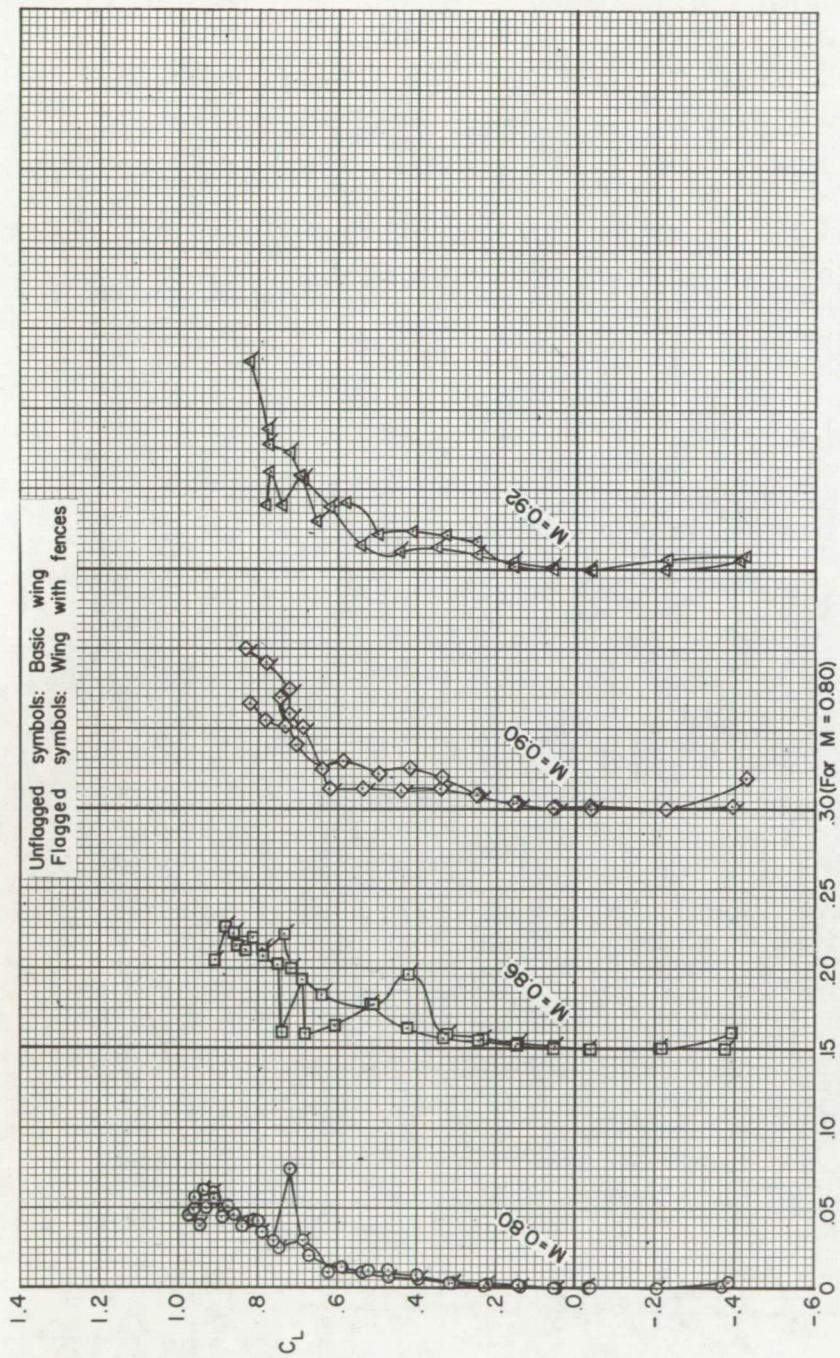

(a) Root-mean-square intensities.

Figure 7.- The effect of fuselage contouring on the fluctuations of wing normal force due to buffet; $\Lambda = 40^{\circ}$.



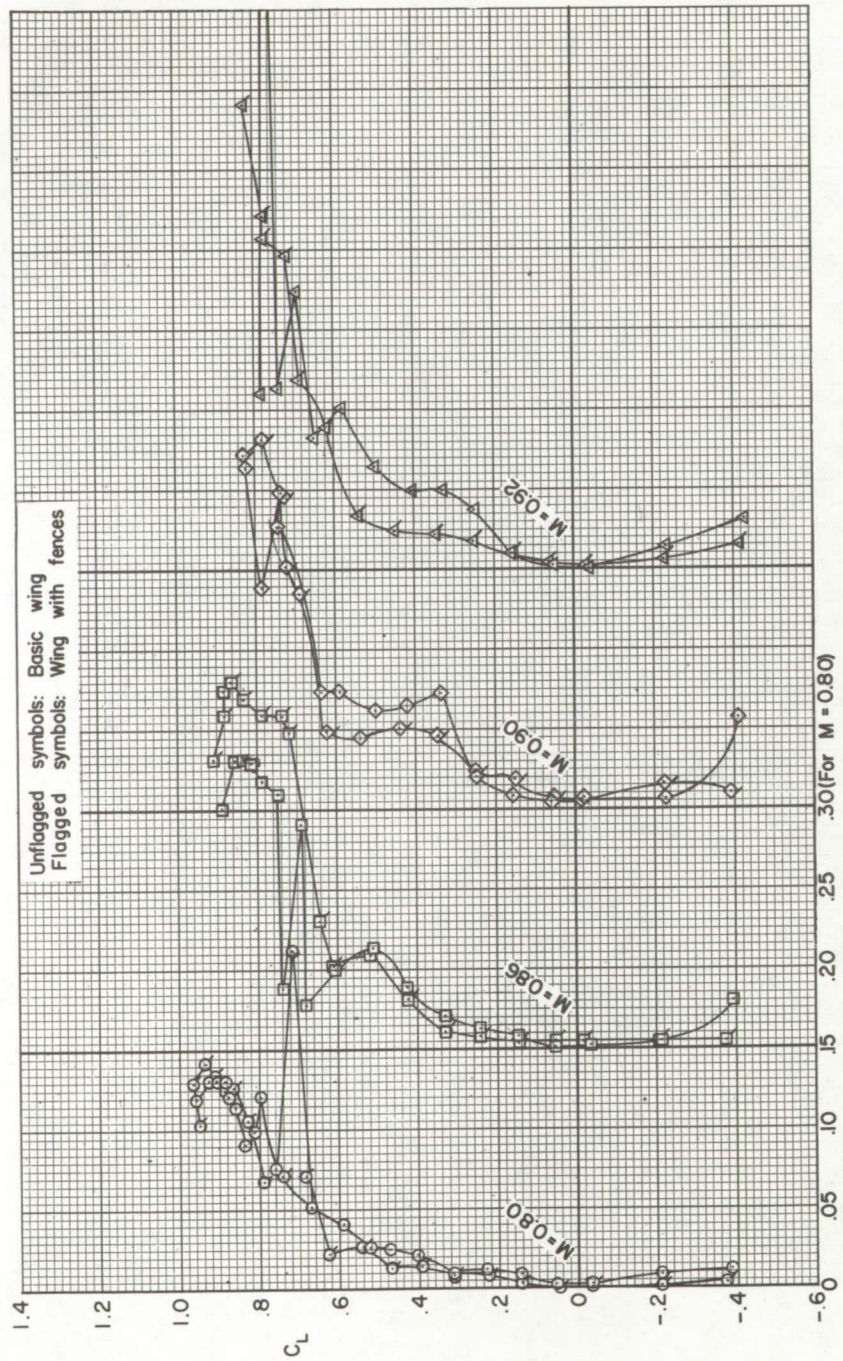

(b) Maximum intensities.

Figure 7.- Concluded.



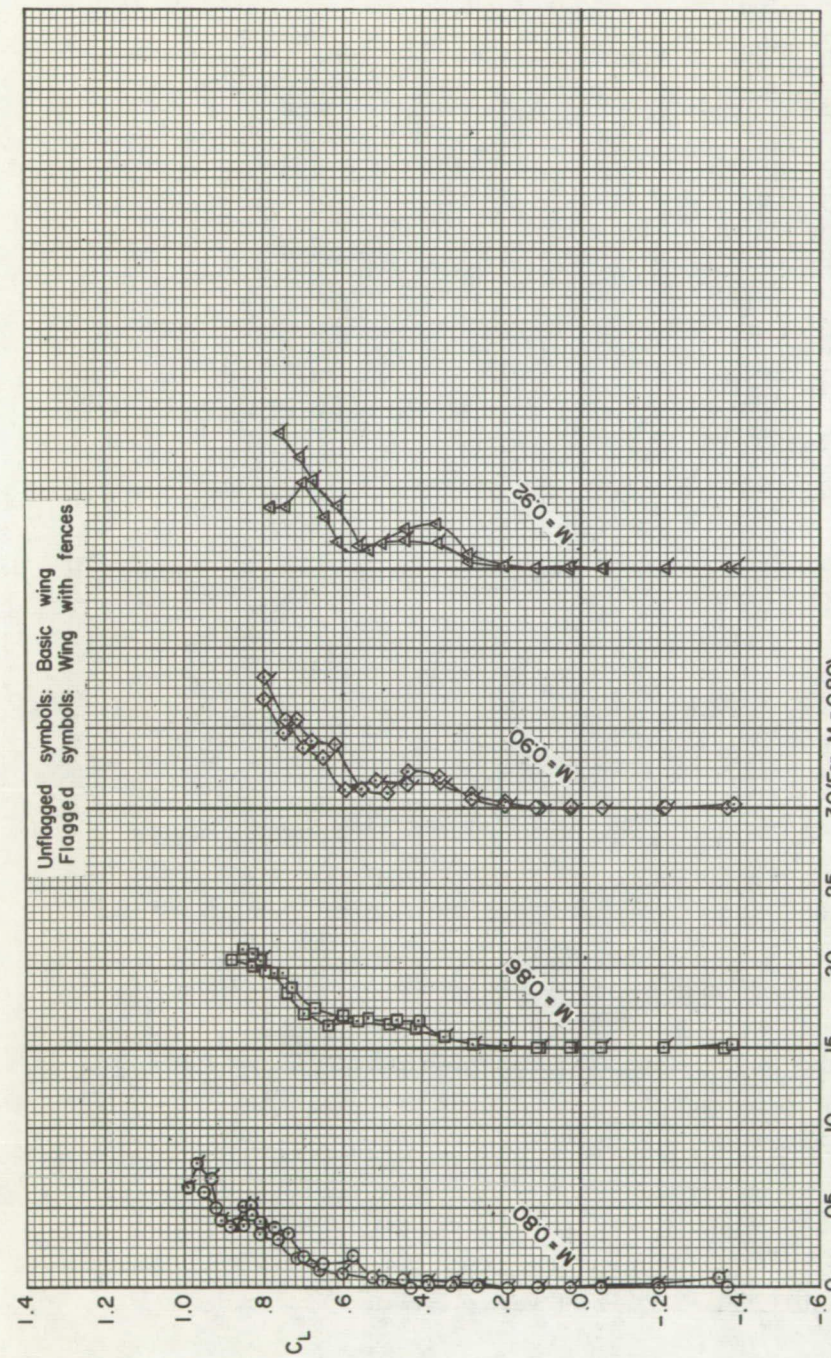

(a) Root-mean-square intensities.

Figure 8.- The effect of wing fences upon the fluctuations of wing normal force due to buffet; $\Lambda = 45°$.



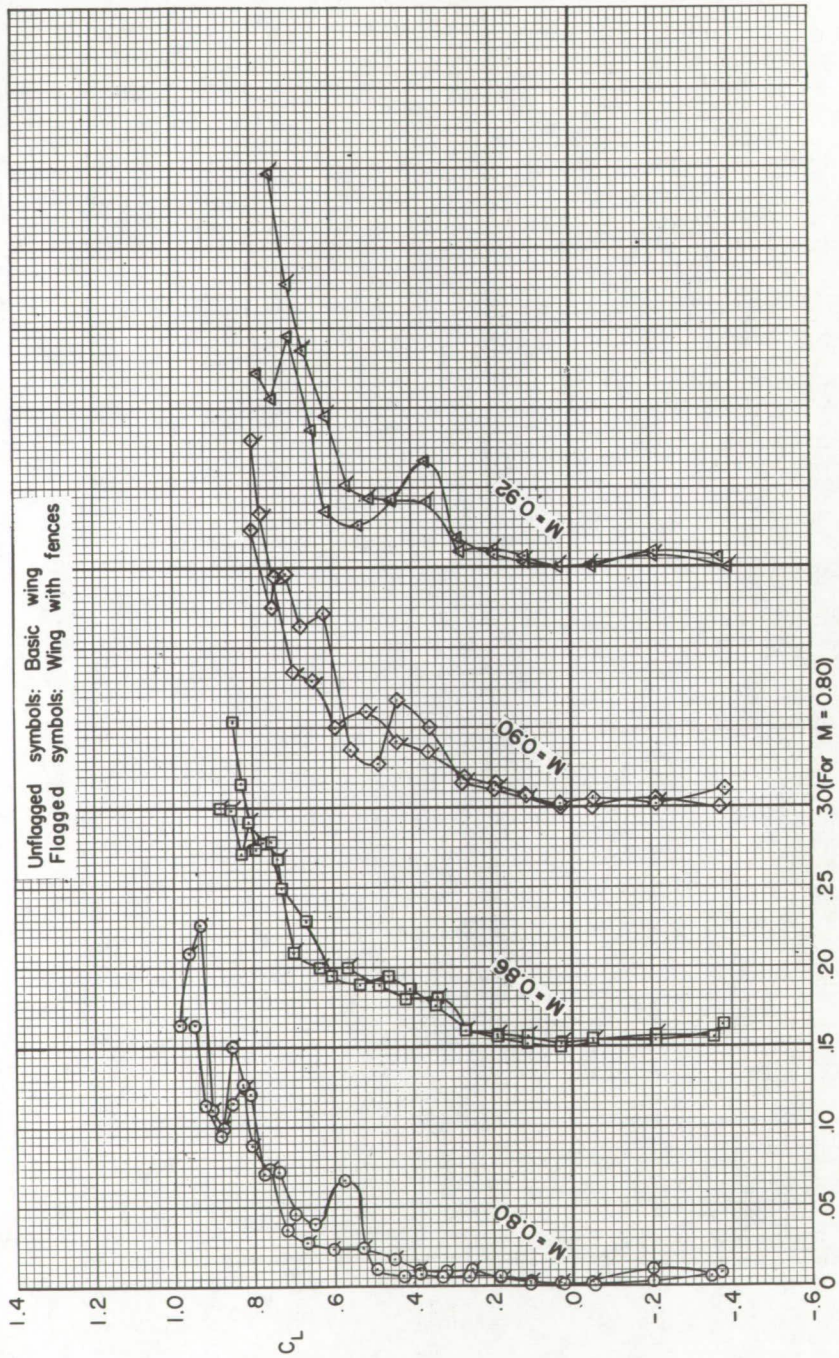

(b) Maximum intensities.

Figure 8.- Concluded.




(a) Root-mean-square intensities.

Figure 9.- The effect of wing fences upon the fluctuations of wing normal force due to buffet; $\Lambda = 50°$.




(b) Maximum intensities.

Figure 9.- Concluded.

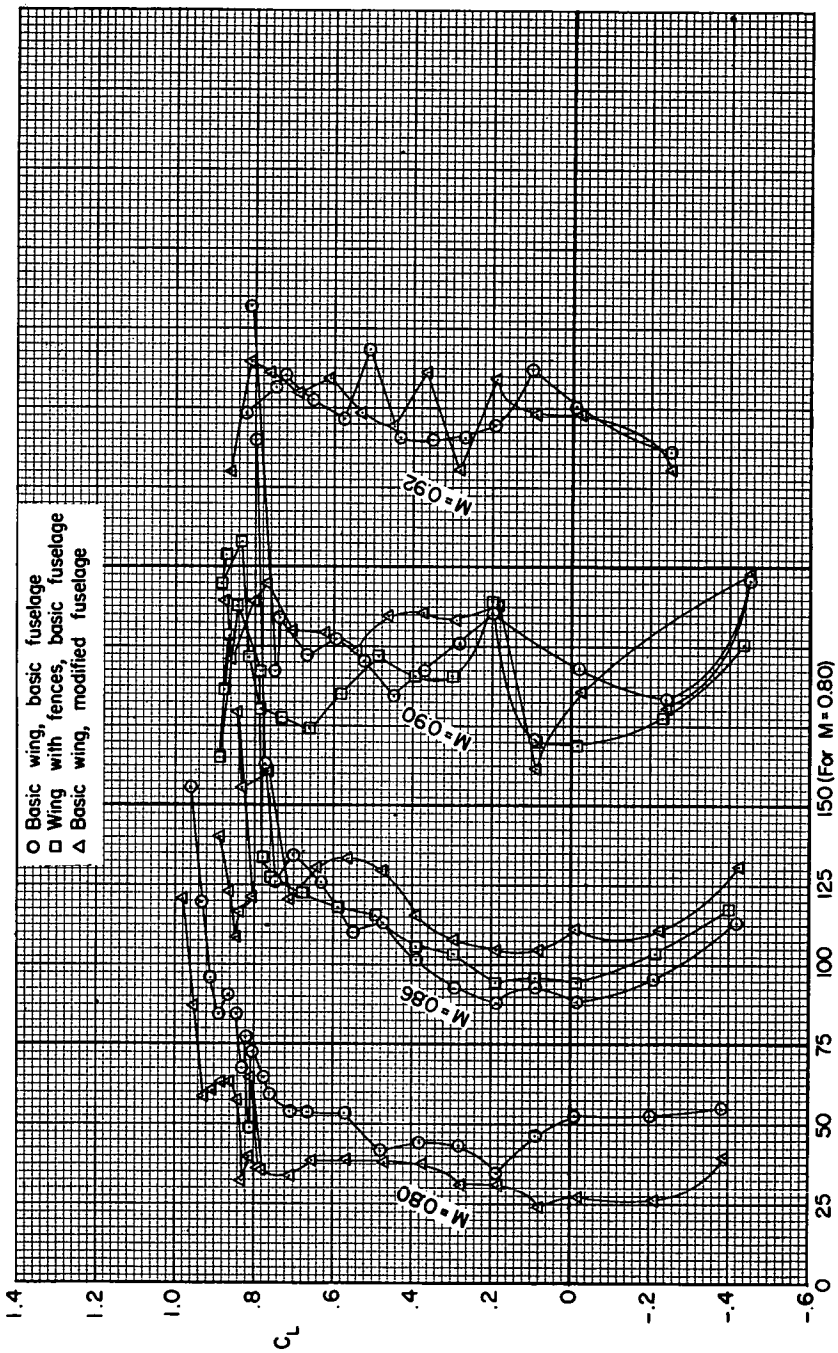



Figure 10.- The effect of wing fences and a fuselage modification on fluctuations of root bending moment of the horizontal tail; tail height = 0(b/2).

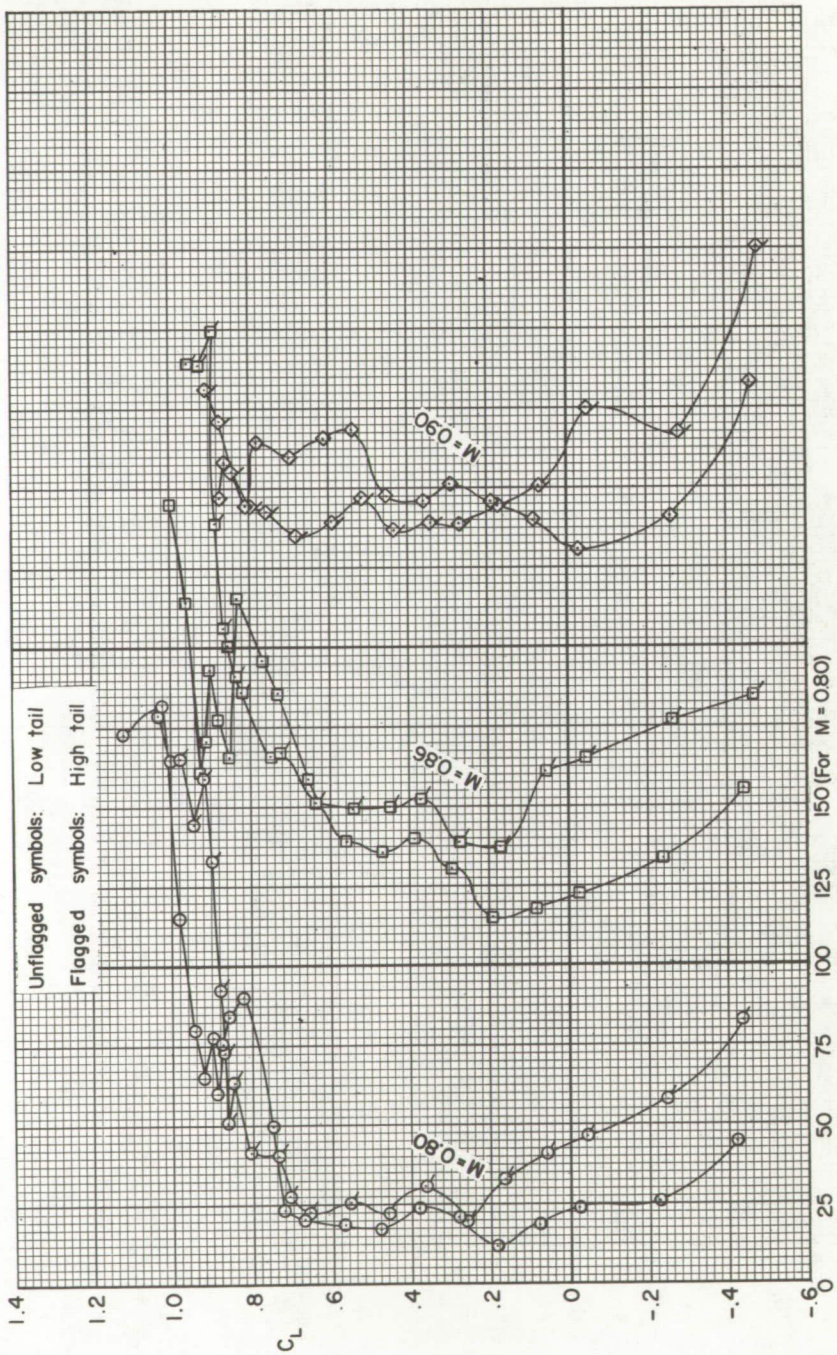
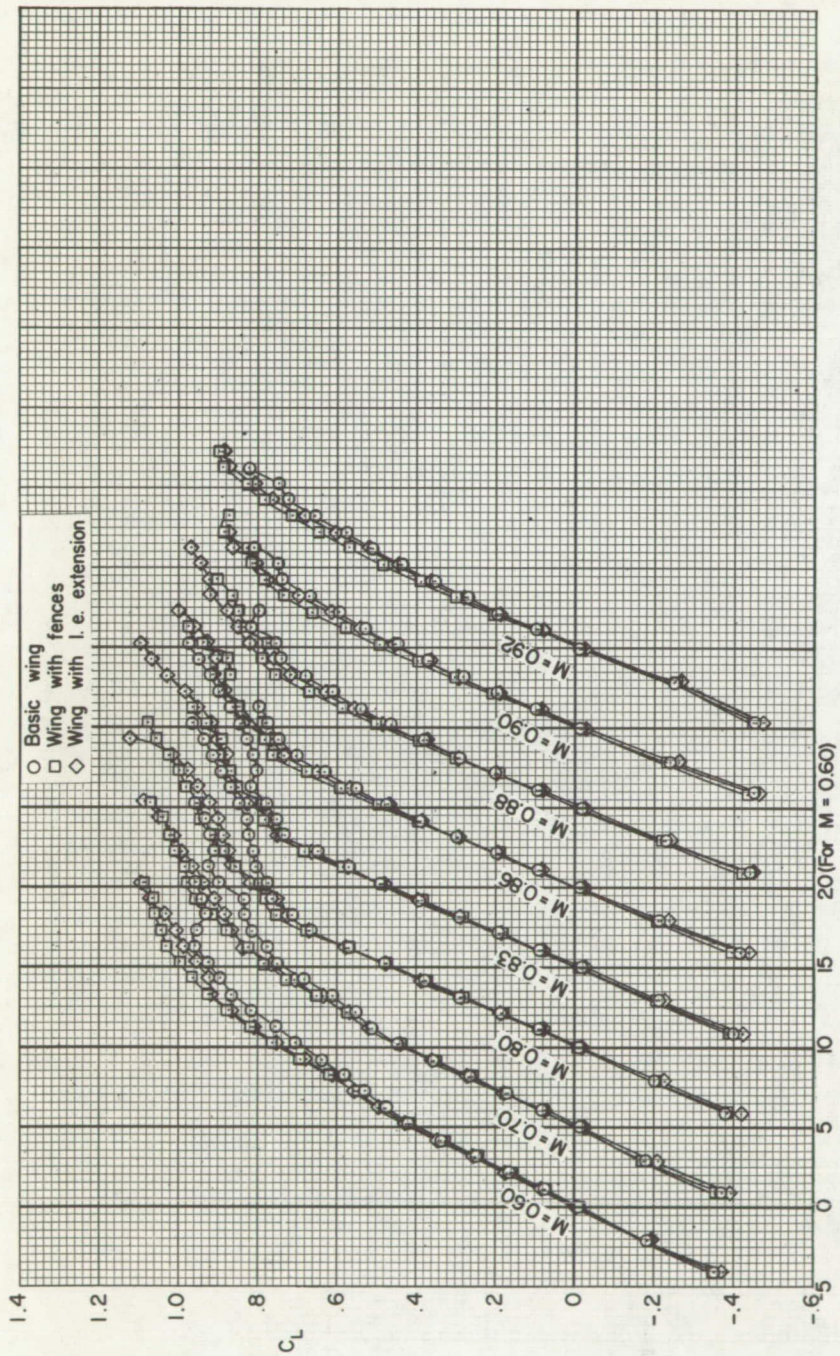
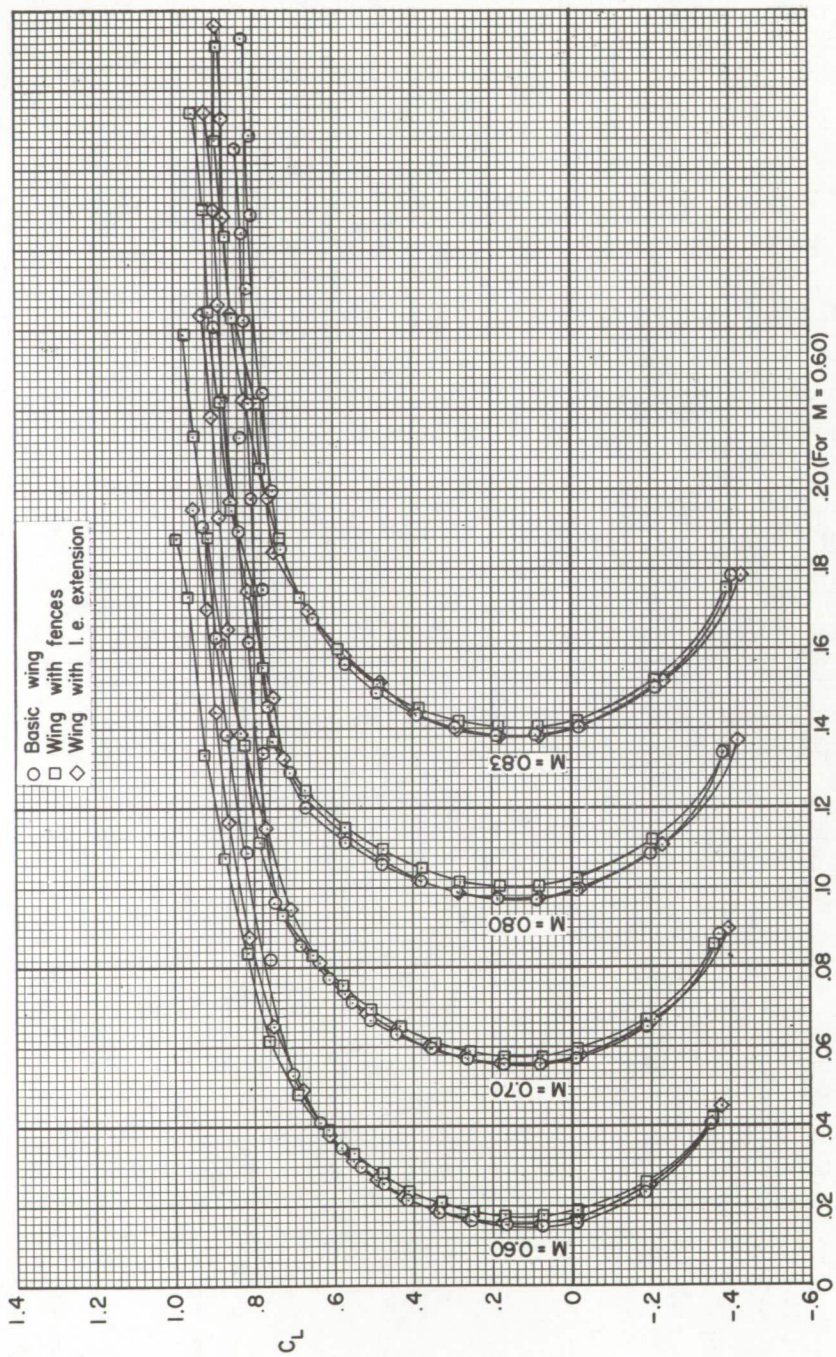



Figure 11.- The effect of tail height on fluctuations of root bending moment of the horizontal tail.



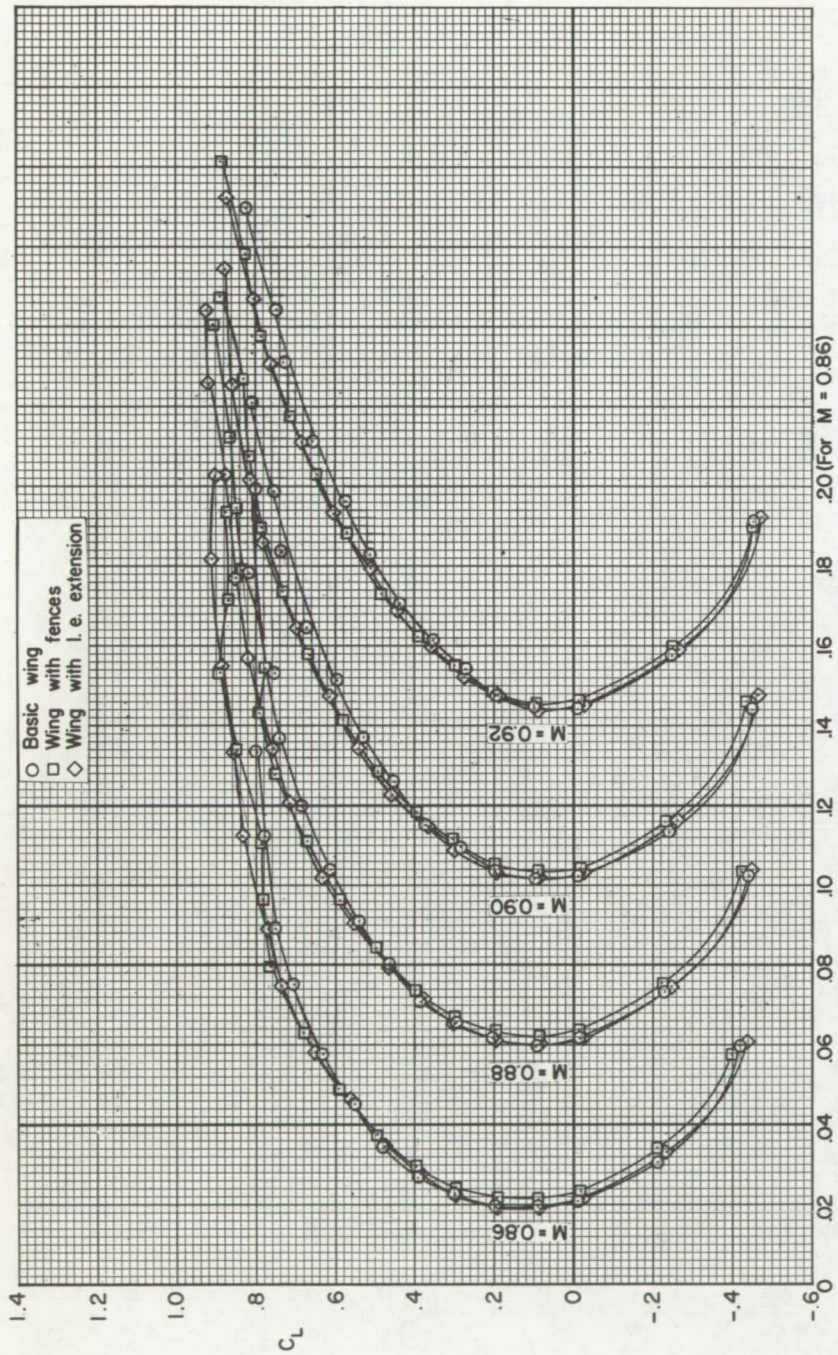

(a) Lift.

Figure 12.- The effect of wing fences and a leading-edge extension upon the longitudinal characteristics of the model with 40° of sweepback.



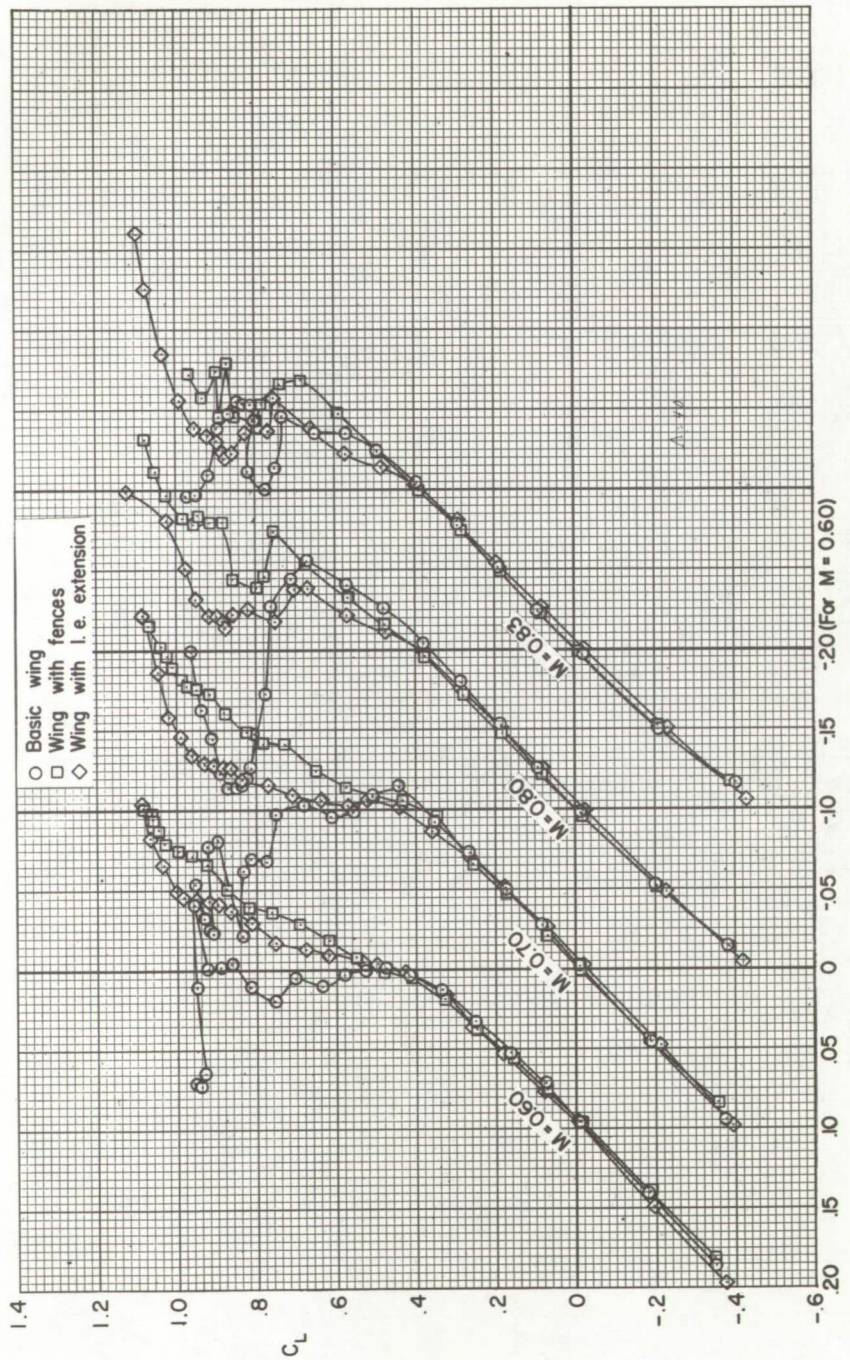

(b) Drag; M = 0.60, 0.70, 0.80, 0.83

Figure 12.- Continued.



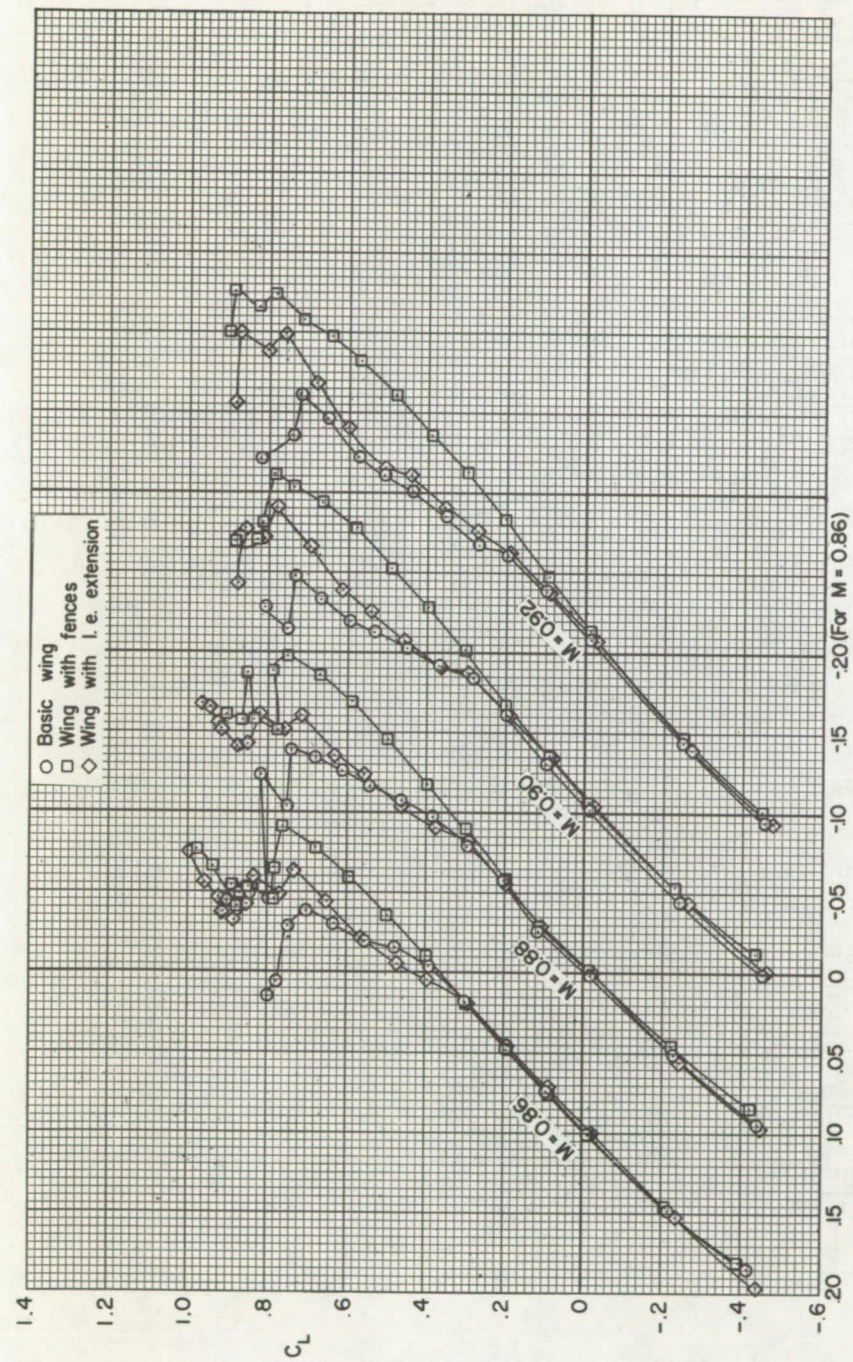

(c) Drag; M = 0.86, 0.88, 0.90, 0.92

Figure 12.- Continued.



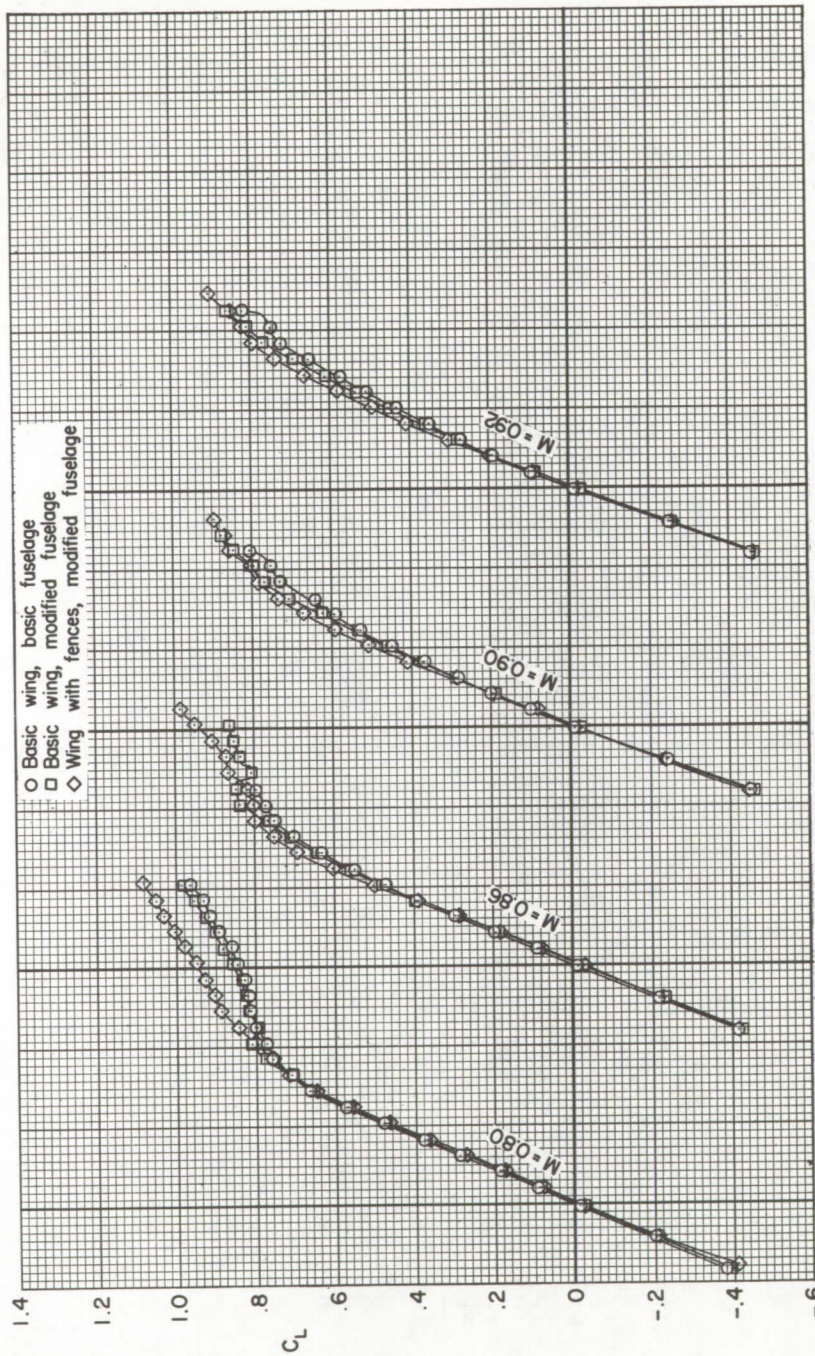

(d) Pitching moment; M = 0.60, 0.70, 0.80, 0.83

Figure 12.- Continued.



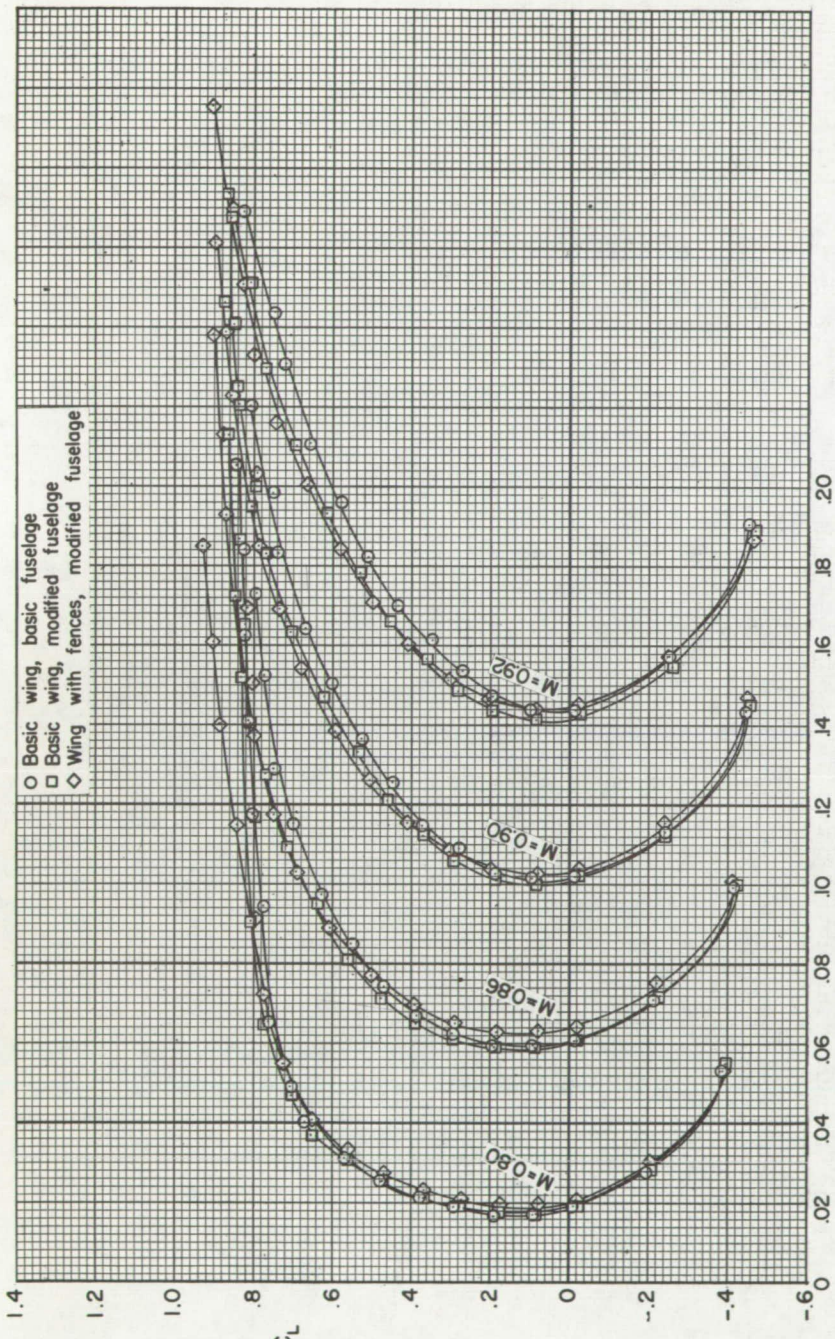

(e) Pitching moment; M = 0.86, 0.88, 0.90, 0.92

Figure 12.- Concluded.



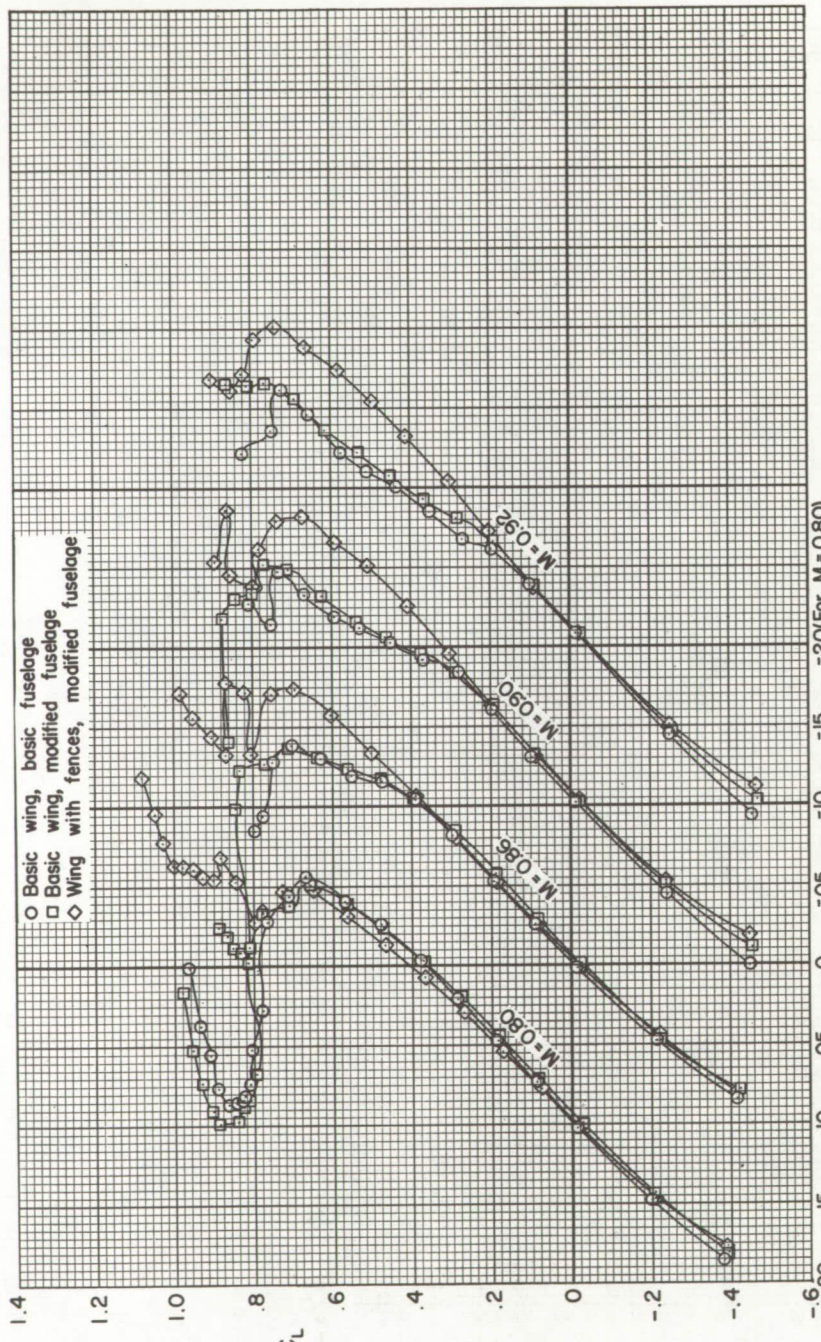

(a) Lift.

Figure 13.- The effect of a fuselage modification and wing fences upon the longitudinal characteristics of the model with 40° of sweepback.



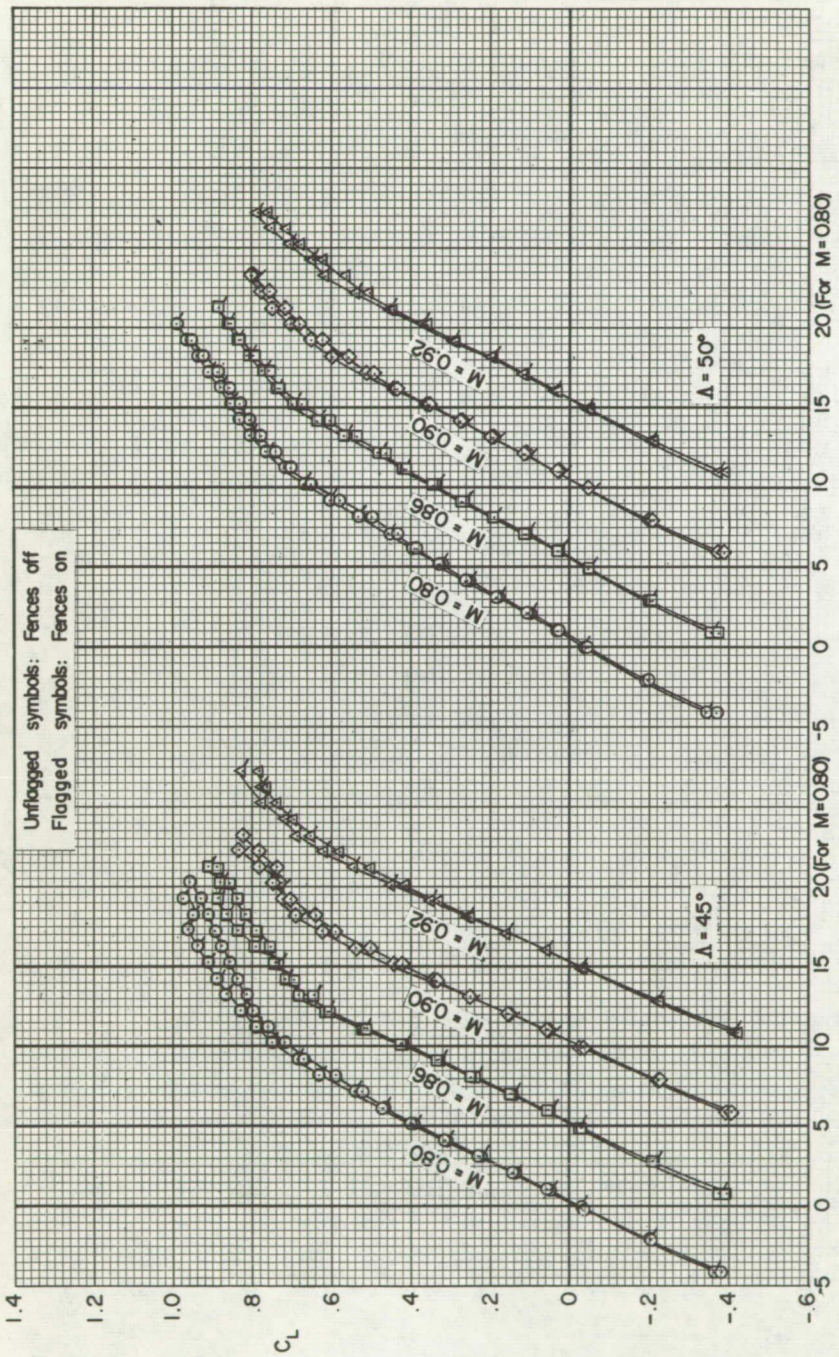

(b) Drag.

Figure 13.- Continued.



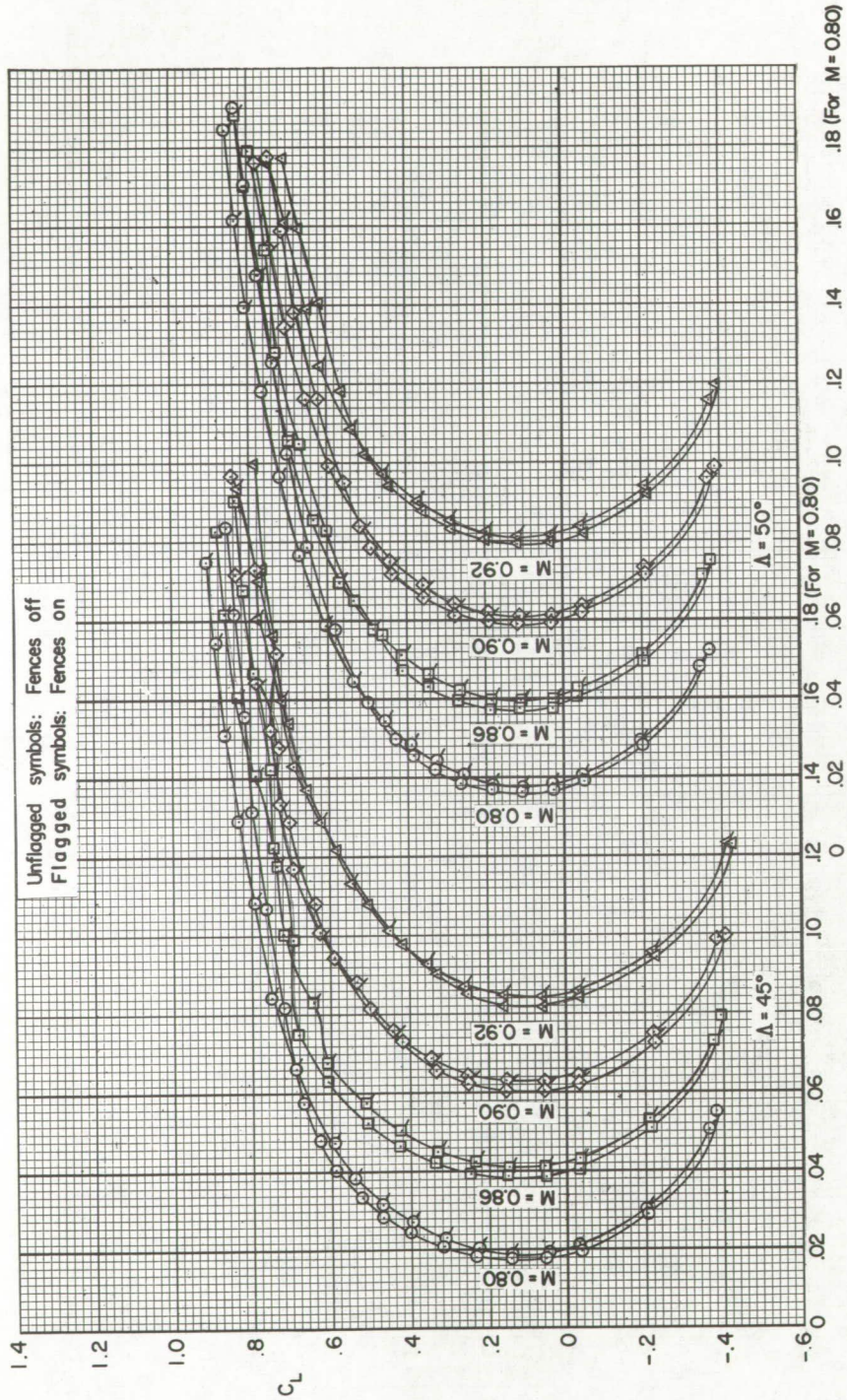

(c) Pitching moment.

Figure 13.- Concluded.



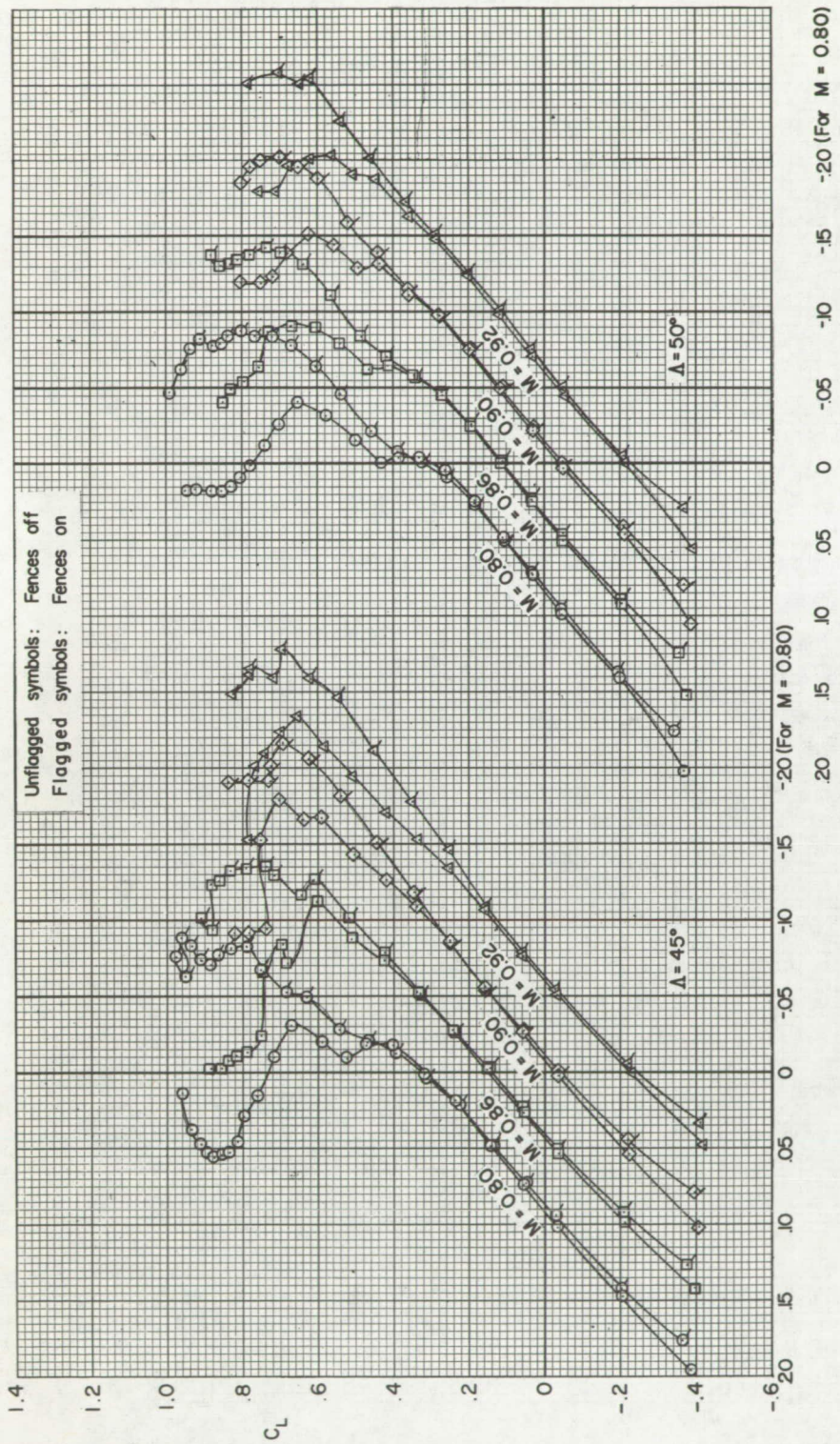

(a) Lift.

Figure 14.- The effect of wing fences upon the longitudinal characteristics of the models with 45° and 50° of sweepback.




(b) Drag.

Figure 14.- Continued.




(c) Pitching moment.

Figure 14.- Concluded.

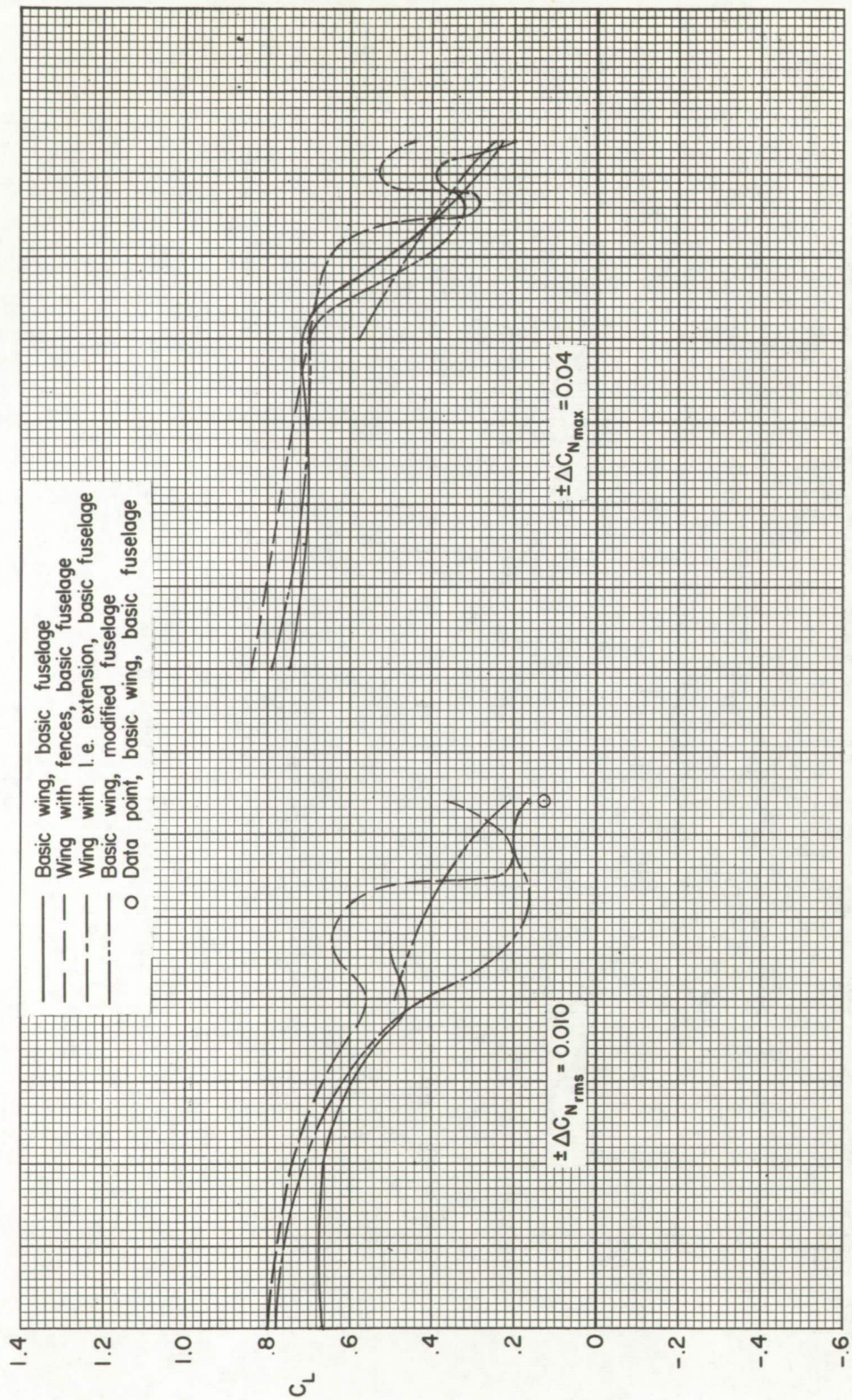
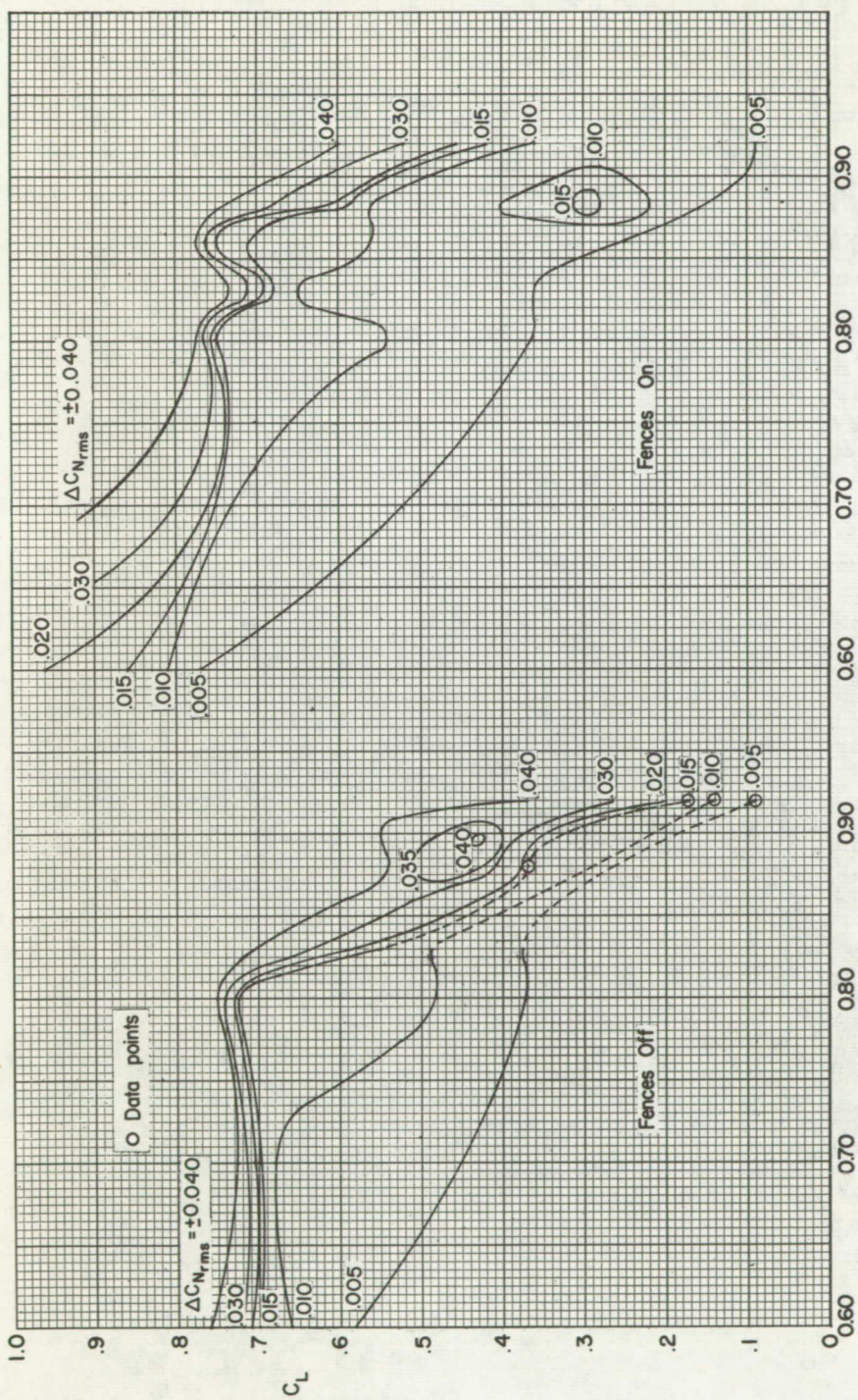
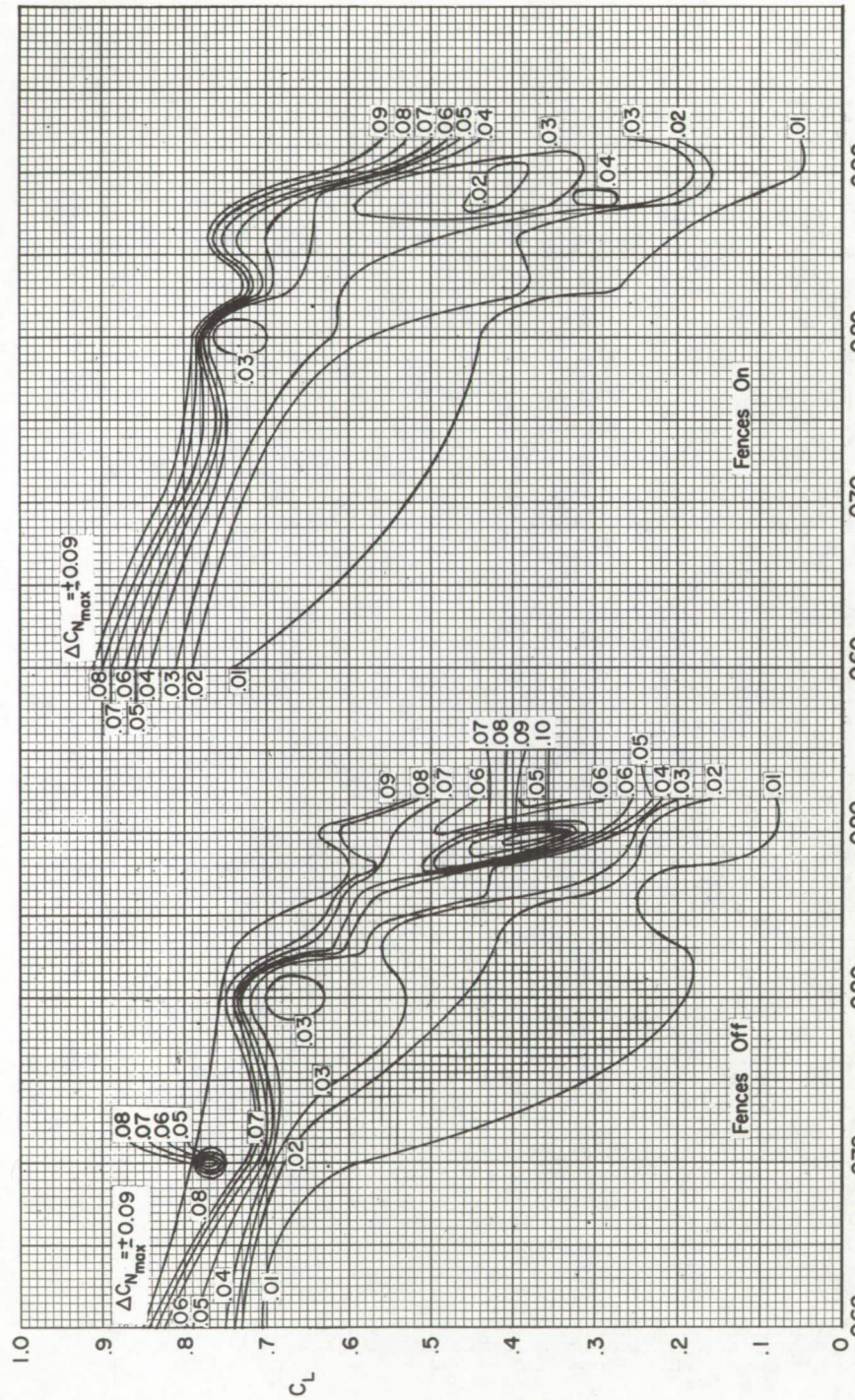



Figure 15.- Boundaries for moderate buffet for the combinations with 40° of sweepback.



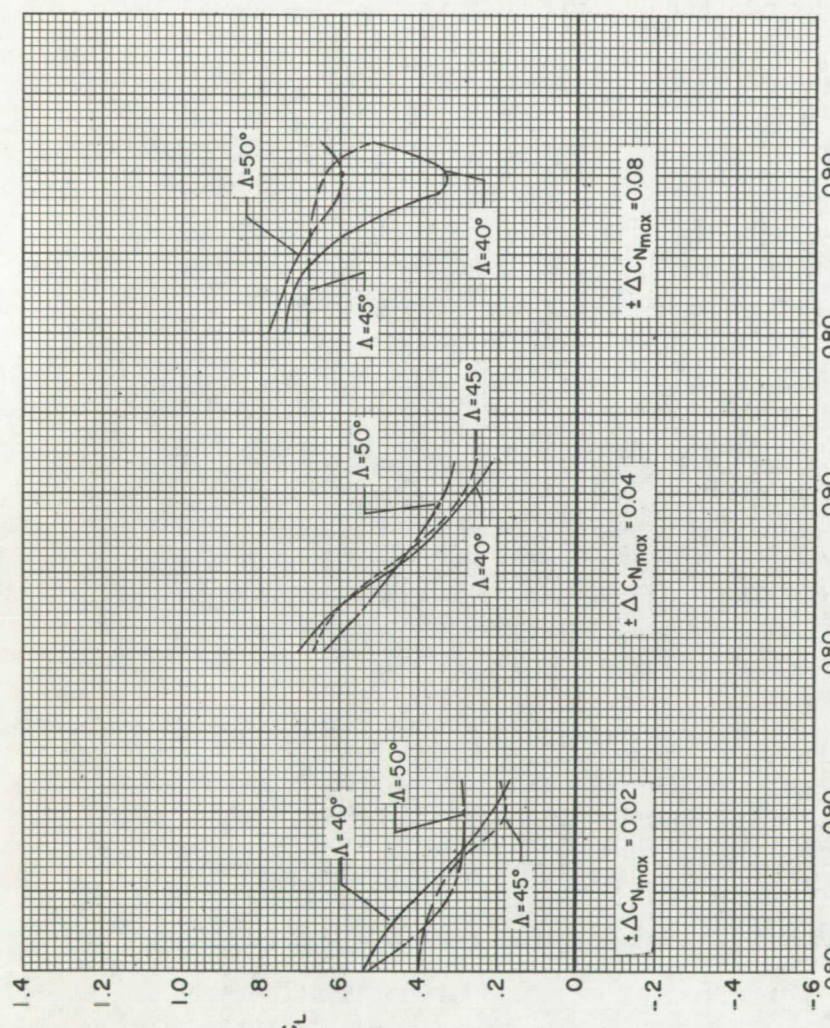

(a) Root-mean-square intensities.

Figure 16.- The variation with Mach number of the boundaries for constant buffet intensities for the combination with 40° of sweepback with and without wing fences.



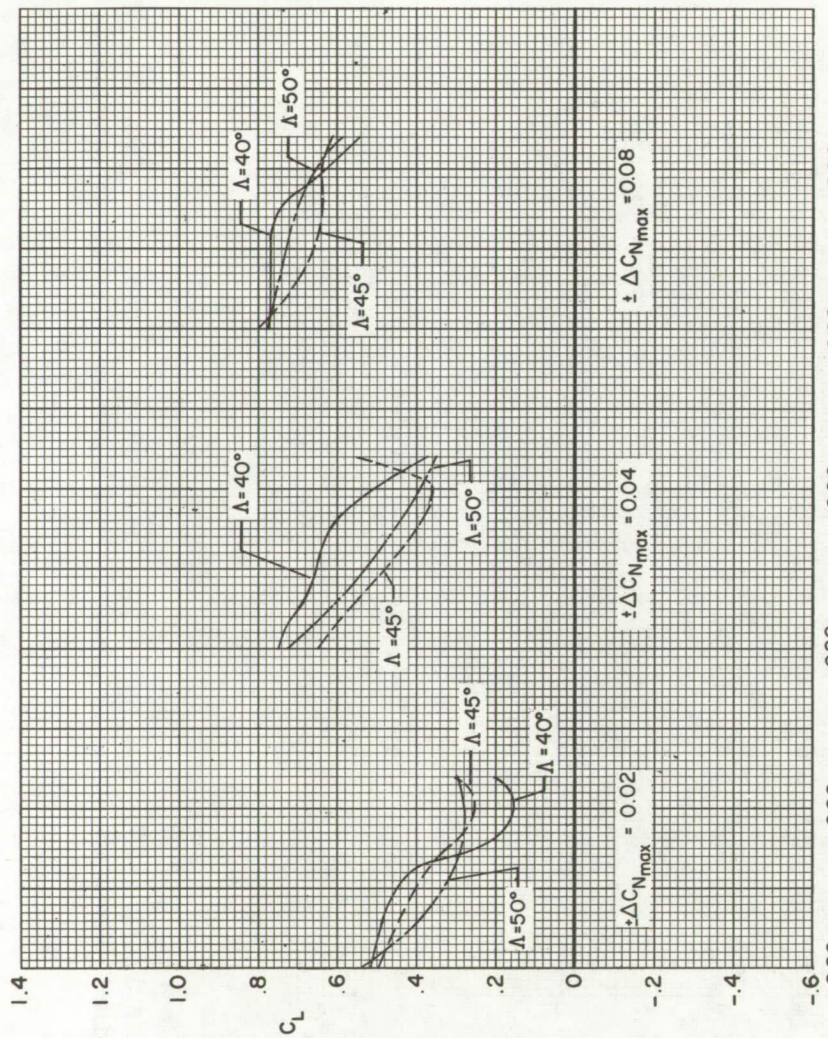

(b) Maximum intensities.

Figure 16.- Concluded.




(a) Fences off.

Figure 17.- The variation with Mach number of boundaries for constant buffet intensities for the combinations with 40°, 45°, and 50° of sweepback; maximum intensities.




(b) Fences on.

Figure 17.- Concluded.

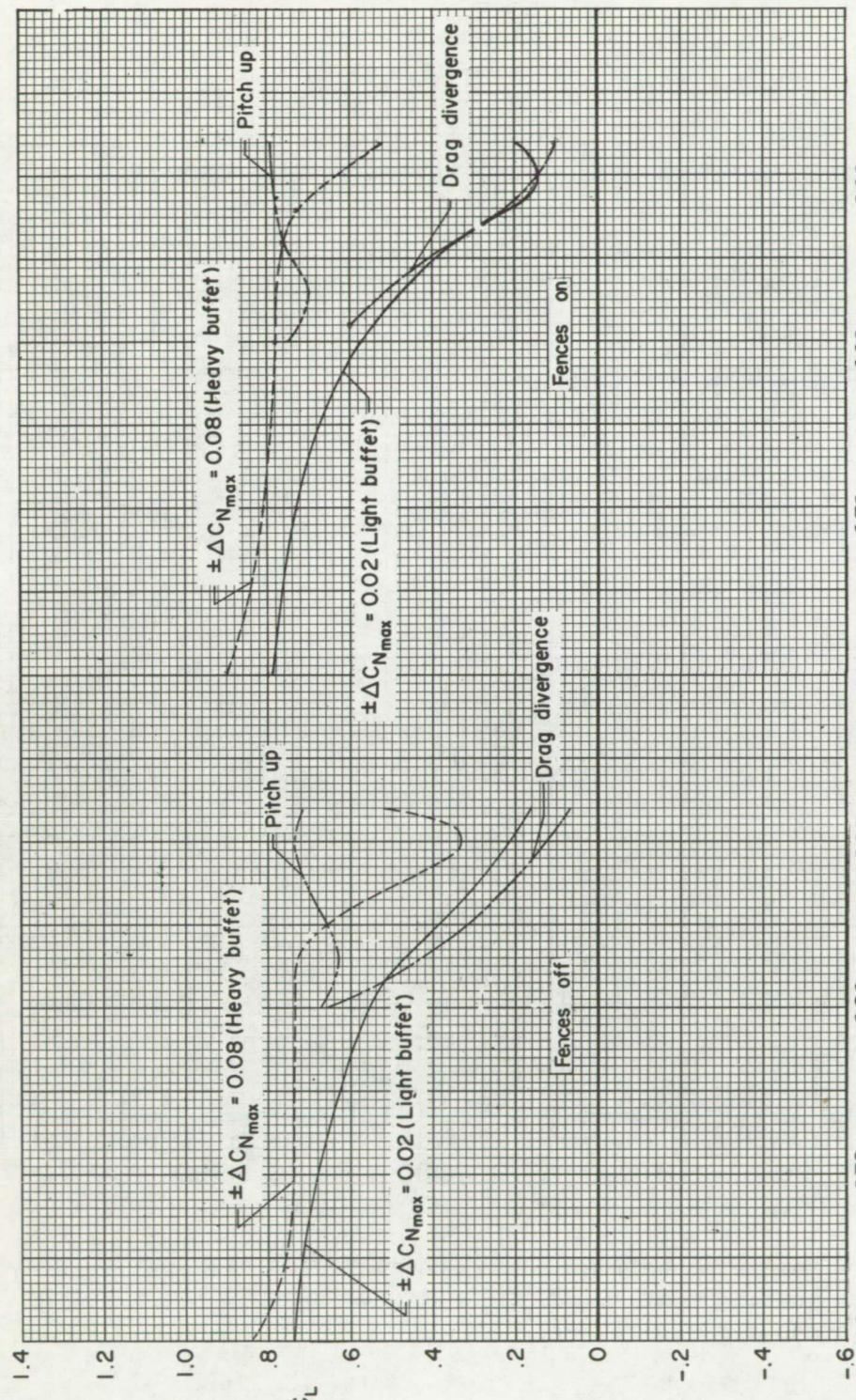



Figure 18.- A comparison of the boundaries for light and heavy buffeting with boundaries for drag divergence and pitch-up for the combination with 40° of sweepback.

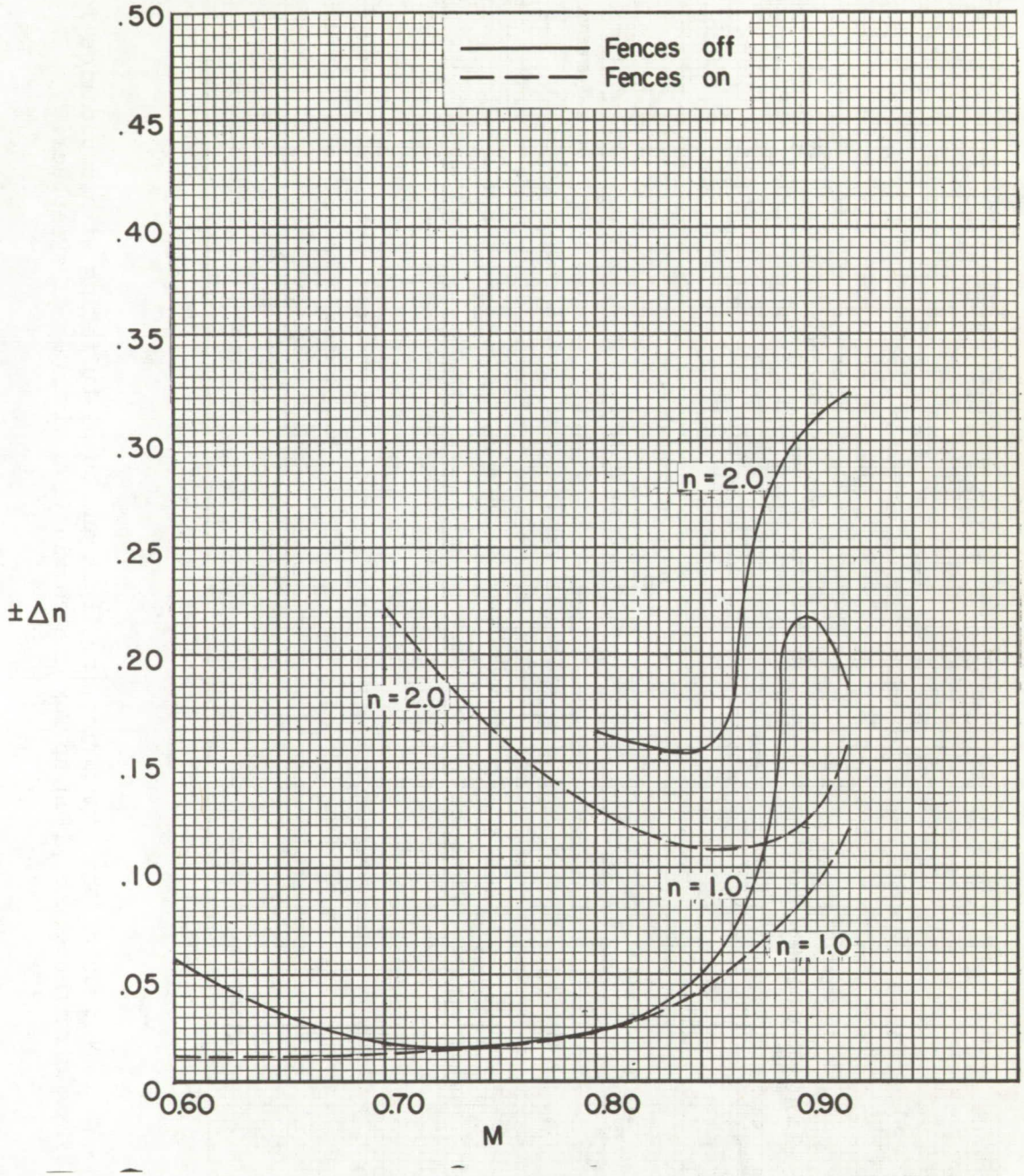



Figure 19.- Some hypothetical buffet characteristics of an assumed airplane in flight at 40,000 feet with an assumed wing loading of 70 pounds per square foot.